NASA TM- 80154

NASA Technical Memorandum 80154

A PARAMETRIC WING DESIGN STUDY FOR A MODERN LAMINAR FLOW WING

FOR REFERENCE

NOT TO BE TAKEN FROM THIS ROOM

JOHN A. KOEGLER, JR.

DECEMBER 1979

NASA

National Aeronautics and
Space Administration

Langley Research Center
Hampton, Virginia 23665

SUMMARY

This report presents the results of a parametric wing design study using the NL(S)-0715F airfoil, a modern laminar flow section. The wings were designed to exhibit desirable stall characteristics while maintaining high cruise performance. It was found that little is sacrificed in cruise performance when satisfying the stall margin requirements if a taper ratio of 0.65 or greater is used. When choosing a taper ratio, however, it must be remembered that the outboard wing loading and thus the wing root bending moment grows with increasing taper ratio.

INTRODUCTION

Since the advent of the airplane, aerodynamicists have constantly tried to increase both its speed and efficiency. The 1930's saw the beginning of a great effort to reduce drag. In order to achieve substantial reductions in drag, many components of the aircraft had to be modified or even reconfigured. The retractable landing gear was introduced along with engine cowling and retractable flaps. Large reductions in parasite drag were obtained by redesigning the aircraft structure such that most, if not all, of the external wires and braces could be removed. Until the 1940's, however, little had been done to reduce the skin friction drag on the wing.

In the 1940's, the National Advisory Committee for Aeronautics (NACA) developed a series of airfoil sections which emphasized laminar flow with good high-speed and reasonable high-lift characteristics. The airfoils which resulted, the NACA 6-digit series, could maintain a laminar flow over much of the surface and exhibited low drag over a reasonable lift range, due to a

1

"favorable pressure distribution. Due to the limitations in both material and fabrication technologies, the wings which were built in the 1940's and 1950's using these sections were not capable of maintaining laminar flow. The wings were covered with aluminum sheeting and were put together with rivets, thus resulting in imperfections which precluded the attainment of laminar flow.

Recent developments in composite structures have made it possible to manufacture a ripple-free wing. One basic problem still surrounding the laminar flow wing centers on what can be done to the design to produce favorable stall characteristics. Since the laminar flow wing must be smooth, it cannot employ stall strips to force an inboard stall, as do many of today's aircraft. The geometry of the laminar flow wing alone must be capable of producing desirable stall characteristics (inboard stall) and hopefully acceptable post-stall dynamics.

The purpose of this report is to present the results of a parametric wing design study using the NL(S)-0715F airfoil, a modern laminar flow section. The series of wings are designed to exhibit desirable stall characteristics while maintaining high cruise performance.

SYMBOLS

AR	Aspect ratio
b	Wing span
c	Reference chord length
$\bar{c}$	Mean aerodynamic chord
C_D	Three dimensional drag coefficient
C_d	Section drag coefficient
C_L	Three dimensional drag coefficient
C_l	Section lift coefficient
$C_{l_{stall}}$	Section lift coefficient at stall

2

C_m Section pitching moment coefficient

C_r Root chord length

C_t Tip chord length

h   Altitude

hp   Horse power

L/D   Lift to drag ratio

M   Mach number

Re   Reynolds number

S   Wing area

x   Distance along chord line as measured from the leading edge

y   Distance along wing semi-span as measured from the root

z   Normal distance from the chord line to the airfoil surface

α Angle of attack

δ_f Flap deflection

λ Taper ratio, C_t/C_r

ANALYSIS METHOD

The NL(S)-0715F Airfoil

The NL(S)-0715F airfoil geometry is pictured in Figure 1. The airfoil is equipped with a plain flap. The airfoil characteristics supplied for this study were calculated at δ_f = -10°, 0°, and 10° and Reynolds numbers of 3, 6, and 9 million using the method of Reference 1. Airfoil data for this section are shown in Figures 2 through 6.

Aircraft Geometry

The geometry of a high performance airplane modeled in this study is presented in Figure 7. The study investigates wings with aspect ratios of 7.89, 10, and 12 for planform areas ranging from 155.2 to 182.6 ft^2. The thickness ratio is held constant at 0.15. Four arbitrary taper ratios were chosen: 0.42, 0.57, 0.65, and 0.75. The taper ratio is defined as the tip

3

chord length divided by the chord length at the centerline of the wing. At each combination of AR, S, and λ, the wing is twisted to achieve the desired stall characteristics. There are no spanwise discontinuities in taper or twist and only full-span flaps are considered.

The wing is mounted 18 inches below the centerline of a 44.8 inch diameter fuselage as is shown in Figure 8. The wing-fuselage angle of incidence is 0°.

Computer Program

The data for this study are derived from a computer program (Reference 2). This program is used to compute the three-dimensional aerodynamic coefficients based on the section data of the NL(S)-0715F airfoil at angles of attack up to and including the estimated stalling angle. This is accomplished by calculating the variation in the downwash along the wing-span. This downwash function is then used to compute the effective angle of attack and two-dimensional aerodynamic coefficients at each of the 20 spanwise stations. These coefficients are then weighted by the area to which they apply and the result is then divided by the wing area to obtain three-dimensional coefficients.

Flight Conditions

Two separate flight conditions are considered. They are:

(1) 65 knots at sea level, and

(2) M = 0.5 at h = 15,000 ft.

For the wings studied, the corresponding Reynolds numbers are approximately 3 and 10 million, respectively.

RESULTS AND DISCUSSION

Wing geometry can be manipulated to vary the stall margin distribution. This is shown in the report by using the method of Reference 2 on wings with AR = 7.89 and S = 155.2 ft^2, but the trends hold true for the complete range of AR and S used in this study. Stall margin is defined as the difference between the effective sectional lift coefficient and the sectional lift coefficient at the stall angle of attack. The spanwise stall margin is a function of many parameters including taper, twist, flap deflection, and Reynolds number. The effect of flap deflections on the stall margin distribution is shown in Figure 9. The wing with undeflected flaps has a more critical or outboard stall than does the wing with a flap deflection of 10°. The variations in the stall margin distribution with changes in Reynolds number, taper, and twist are illustrated in Figures 10, 11, and 12, respectively. The stall moves inboard with increasing Reynolds numbers. The stall can also be moved inboard by increasing either the taper ratio or the washout.

The stall margin distribution selected for use in this study (Reference 2) is presented in Figure 13. The criterion for arriving at a distribution such as this is that the stall margin should be approximately 0.1 at 70 percent of the semi-span. This criterion insures that the stall will occur inboard first. It was shown that the wing with undeflected flaps operating at a Reynolds number of approximately 3 million has the most critical stall margin distribution. By adding the proper amount of twist to this wing, the desired stall margin distribution can be obtained. The amount of twist required at each taper ratio in order to obtain the desired spanwise stall margin

distribution is presented in Figure 14. By forcing the stall margin distribution of this particular wing onto the desired curve, the stall margin distribution of all the wings considered become acceptable.

With these trends established, the planform area is now varied between 155.2 and 182.6 ft^2. The maximum L/D is found to increase approximately linearly (due to increases in span) with increasing planform areas as is shown in Figure 15. The cruise efficiency, therefore, is improved by increasing S. The efforts of this study, therefore, will now be concentrated on wings with S = 182.6 ft.

The taper-twist combinations which produce a stall margin of 0.1 at $2y/b = 0.7$ for a wing whose AR = 7.89 and S = 182.6 ft^2 are shown in Figure 16. Once again a linear relationship is seen between the taper and twist required to obtain the desired stall margin.

The variation in $(L/D)_{max}$ with taper for Reynolds numbers of approximately 3 and 10 million is shown in Figure 17. When maintaining the desired stall margin, it is seen that $(L/D)_{max}$ increases nonlinearly with increasing taper ratios. If, however, the stall margin is sacrificed in search for the largest $(L/D)_{max}$, then $(L/D)_{max}$ is found to increase linearly with decreasing taper ratios. This figure shows that a substantial penalty in $(L/D)_{max}$ is a accrued in order to achieve the desired stall margin with lower taper ratios, whereas little is sacrificed in $(L/D)_{max}$ at taper ratios of 0.65 to 0.75. Finally, these curves are compared with the case in which the wing drag is based on the ideal polar $(C_D = C_{d_{wing_{min}}} +$

$C_{D_{fuselage \ and \ tail}} + \dfrac{C_L^2}{\pi \ AR})$. That is, the drag calculation was made by

assuming an eliptical load distribution and by using the minimum C_d (see Figure 4) over the full range of C_l's.

The loading distributions for several wings that satisfy the desired stall margin and in which AR = 7.89 and S = 182.6 ft^2 are given in Figure 18. The wing loading curves become flatter with increasing taper ratios. This suggests that the outboard forces and thus the wing root bending moments are much greater on wings with high taper ratios.

The effect of wing area on the performance will now be examined. The power required curves for wings with S = 155.2, 170, and 182.6 ft^2 are presented in Figure 19. These curves apply to wings which have no twist, a taper ratio of 0.75, and operate at a Reynolds number of approximately 3 million. As can be seen in Figure 19, the stall speed is reduced from 64 to 59 knots as S is increased from 155.2 to 182.6 ft^2. The (flight) endurance of the aircraft also lengths with increasing S, due to increases in the wing span.

The power curves for the same wings operating at a Reynolds number of approximately 10 million are presented in Figure 20. The curves show that the penalty for increasing S to 182.6 ft^2 is approximately 6 knots for a given hp in the 200 to 300 knot range. Assuming a desire for reduced fuel consumption, it appears that more is gained than is sacrificed when S is increased (within the wing area range considered).

The trends which were established with AR = 7.89 apply for AR = 10 and 12 as well. The data for wings with AR = 10 and 12 are presented in Figures 21 through 30.

Finally, the effect of AR on the performance is now studied. The remaining figures apply to wings with $S = 182.6$ ft^2 and $\lambda = 0.75$. The maximum L/D is greatly affected by changes in AR, as is seen in Figure 31. In Figure 31, three separate curves are shown: one in which the $(L/D)_{max}$ is sacrificed for the required stall margin; another in which the wing was twisted to find the largest possible $(L/D)_{max}$ regardless of the stall margin; and the last curve represents the $(L/D)_{max}$ if calculated using

$$C_D = C_{d_{wing_{min}}} + C_{D_{fuselage\ and\ tail}} + \frac{C_L^2}{\pi\ AR}.$$ This figure emphasizes that

little or nothing is lost in $(L/D)_{max}$ when satisfying the stall margin requirements if a taper ratio of 0.75 is used. Finally, the penalty for not having an eliptically loaded wing which operates at the minimum C_d can be realized.

The effect of AR on the stall speeds and cruise efficiency is shown in the power curves which are presented in Figure 32. These curves are for wings which operate at $Re = 3 \times 10^6$ and which satisfy the stall margin requirements. The cruise efficiency is greatly improved by increasing the aspect ratio. The stall speeds, however, are unaffected by changes in AR. The stall speeds are reduced by 3 knots when the flaps are deflected to 10°.

Higher aspect ratios not only improve cruise performance, but require no additional power at high speeds as well. This can be seen in Figure 33. Figure 33 also shows the decrease in power required at high speeds if $\delta_f = -10°$.

8

CONCLUDING REMARKS

Since the laminar flow wing must be smooth, the desired stall characteristics must be produced solely by the wing geometry. This report presents the results of a parametric wing design study using the NL(S)-0715F airfoil, a modern laminar flow section. The wings were designed to exhibit desirable stall characteristics while maintaining high cruise performance. It was shown that many geometries can provide these stall characteristics, but that certain geometries yield superior performance. It was found that little is lost in cruise performance when satisfying the stall margin requirements if a taper ratio of 0.65 or greater is used. When choosing a taper ratio, however, it must be remembered that the wing root bending moment grows with increasing taper ratios.

REFERENCES

1. Eppler, R.: Direct Calculation of Airfoils From Pressure Distribution.
   NASA TT F-15417, 1974.

2. McVeigh, M. A.; and Kisielowski, E.: A Design Summary of Stall
   Characteristics of Straight Wing Aircraft. NASA CR-1646, June 1971.

10
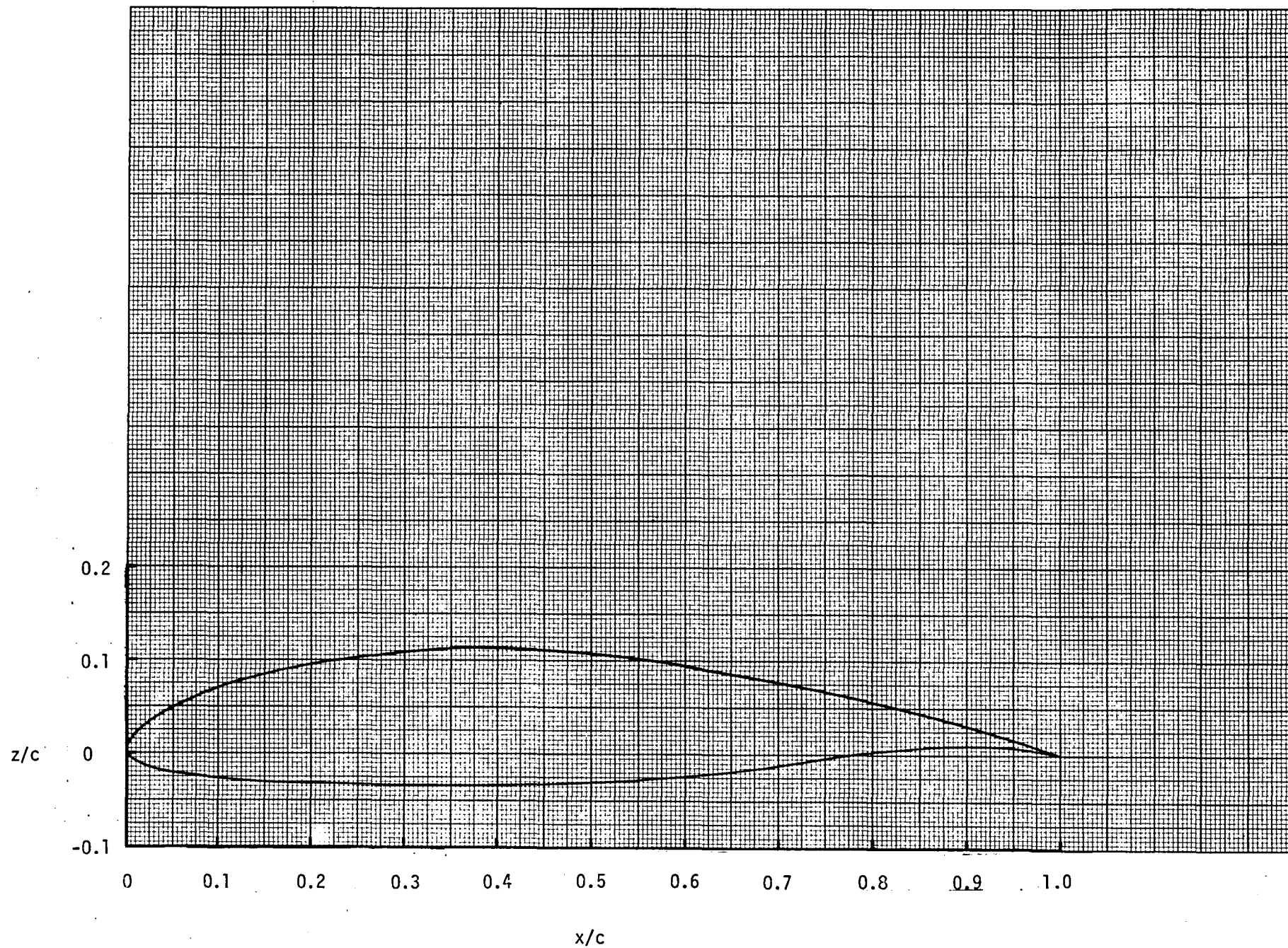
Figure 1. - The NL(S)-0715F airfoil geometry.
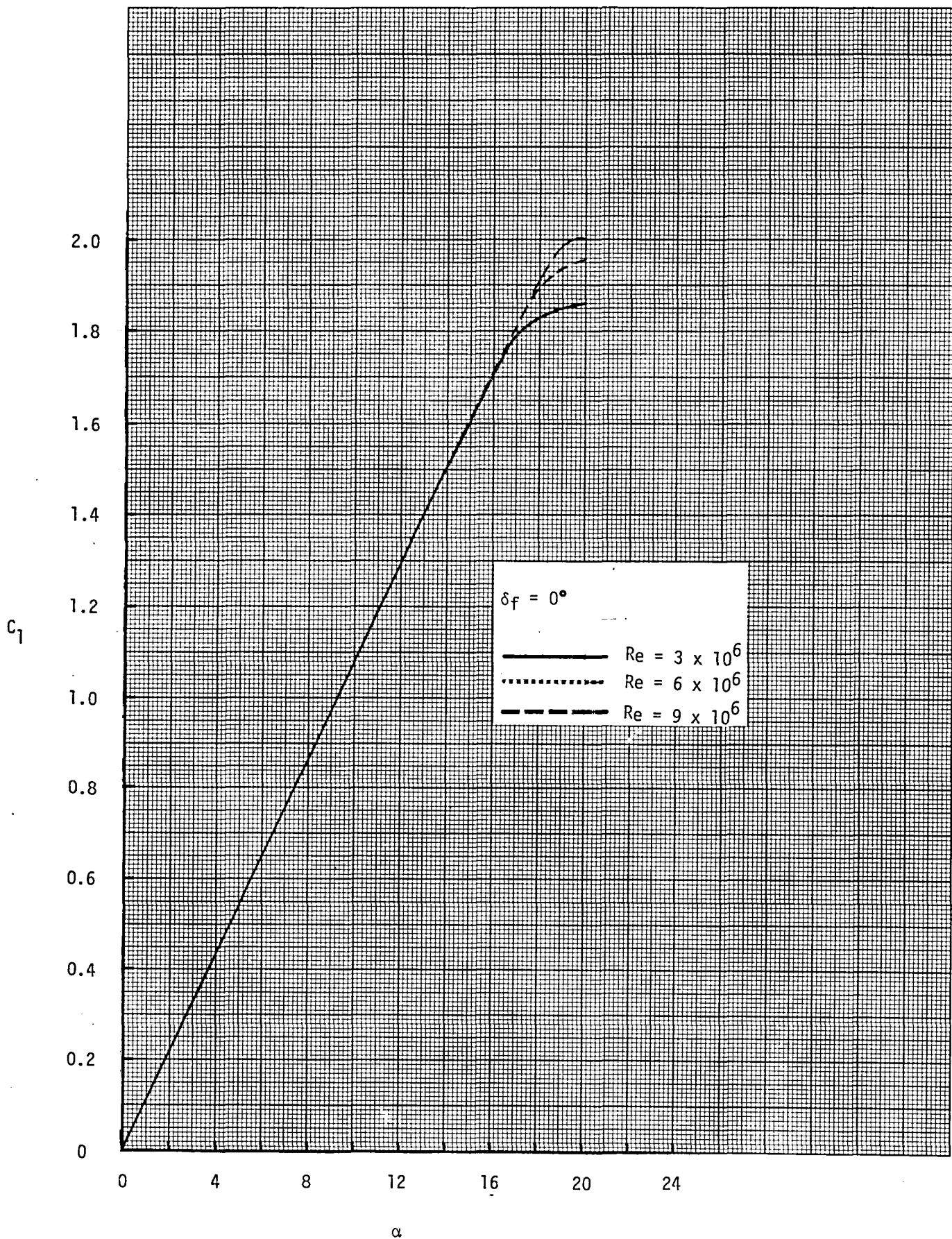
Figure 2. - Section lift coefficient as a function of the absolute angle of attack for the NL(S)-0715F airfoil with $\delta_f = 0°$.
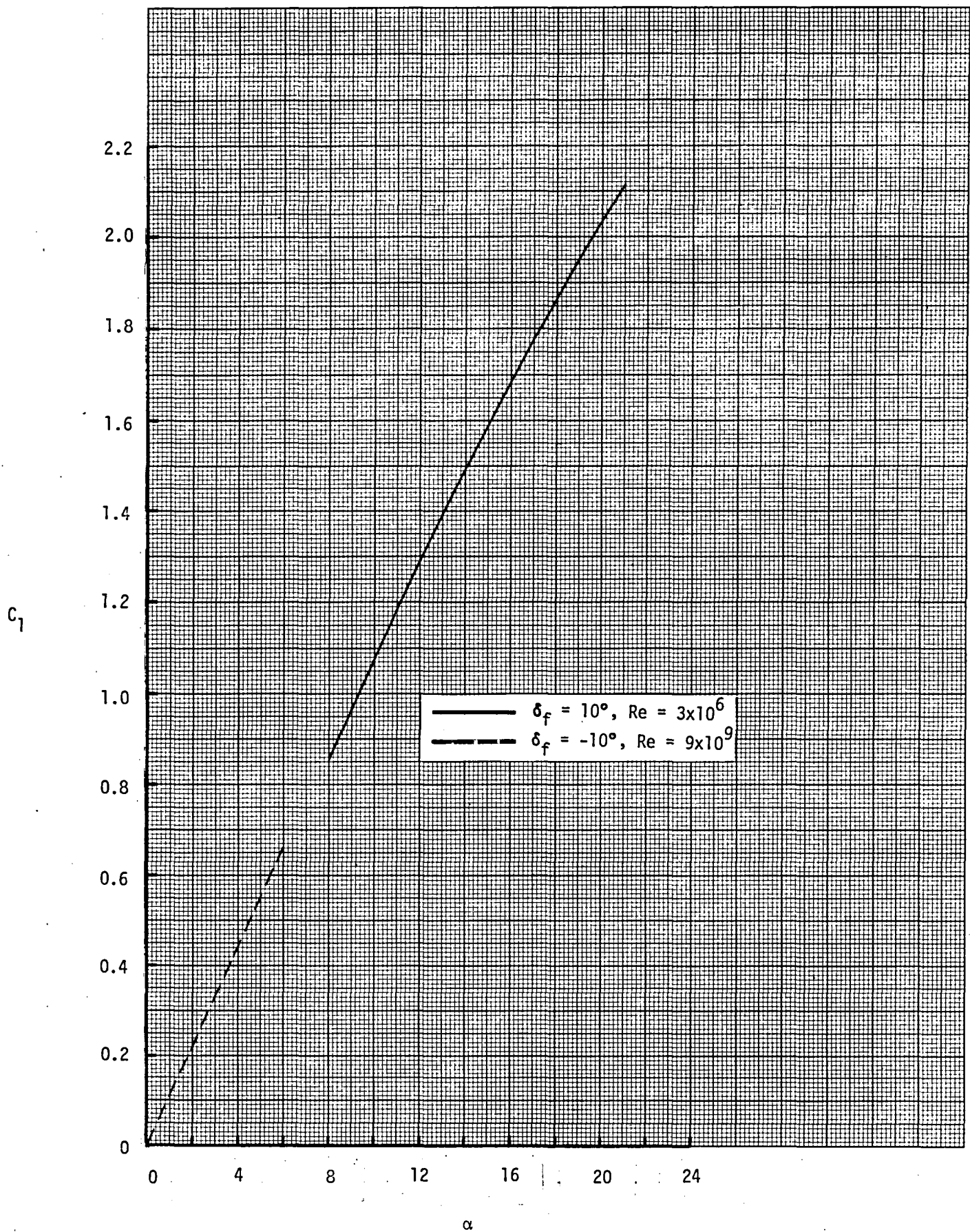
Figure 3. - Section lift coefficient as a function of the absolute angle of attack for the NL(S)-0715 airfoil with $\delta_f = -10°$ and 10°.
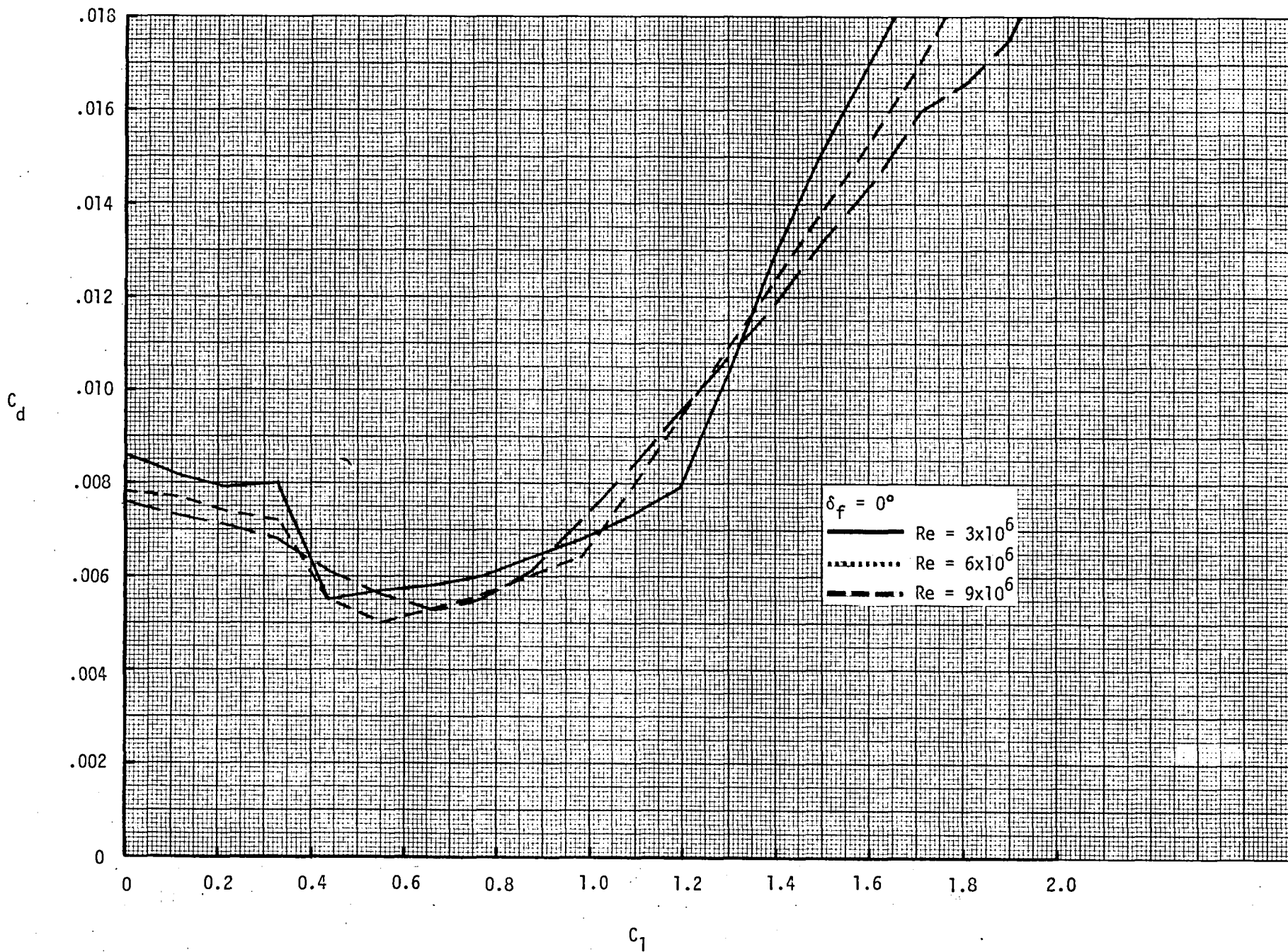
Figure 4. – Two dimensional drag polars of the NL(S)-0715F
airfoil with $\delta_f = 0°$.
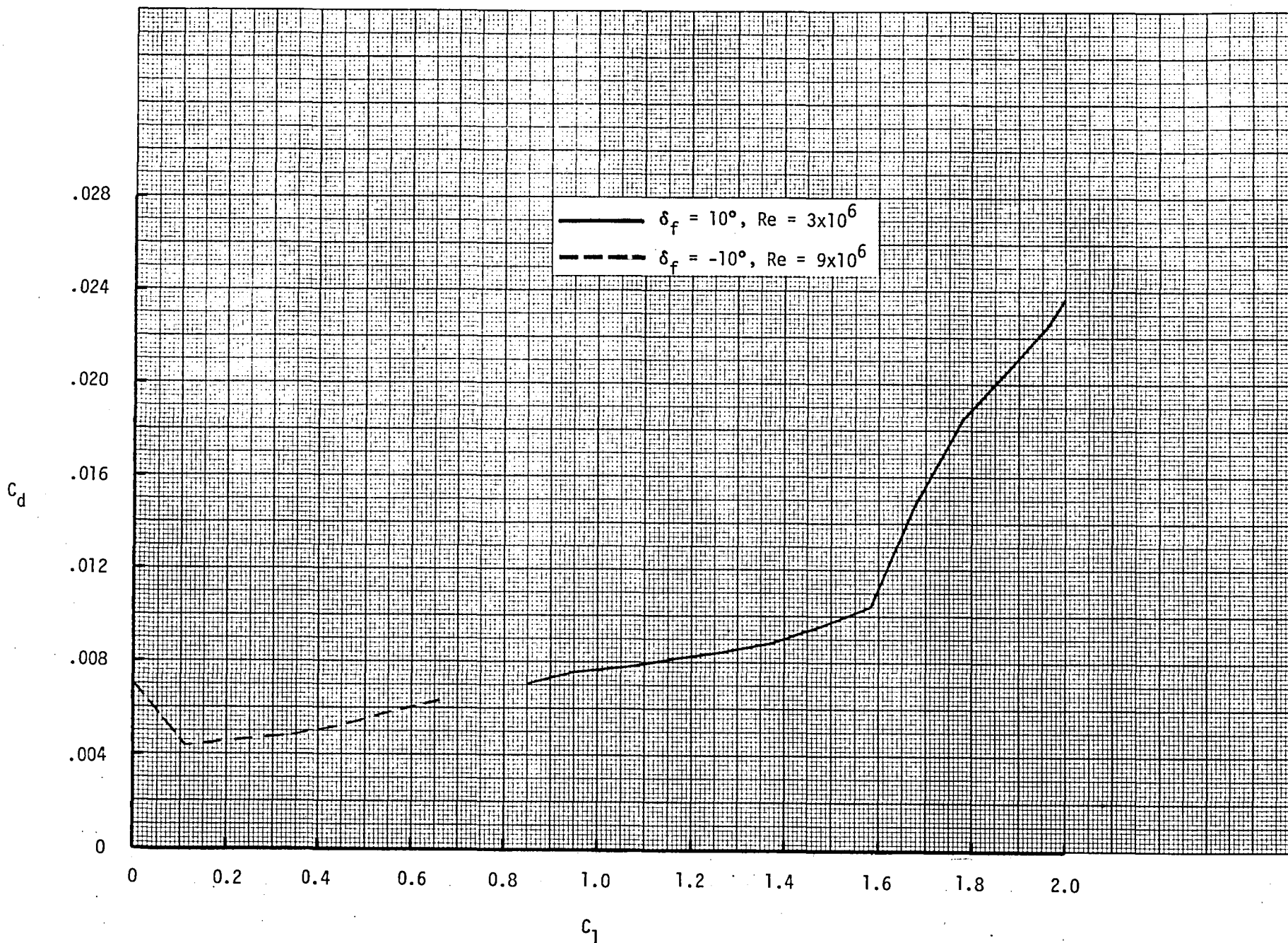
Figure 5. - Two dimensional drag polars of the NL(S)-0715F airfoil
with δ_f = -10° and 10°.
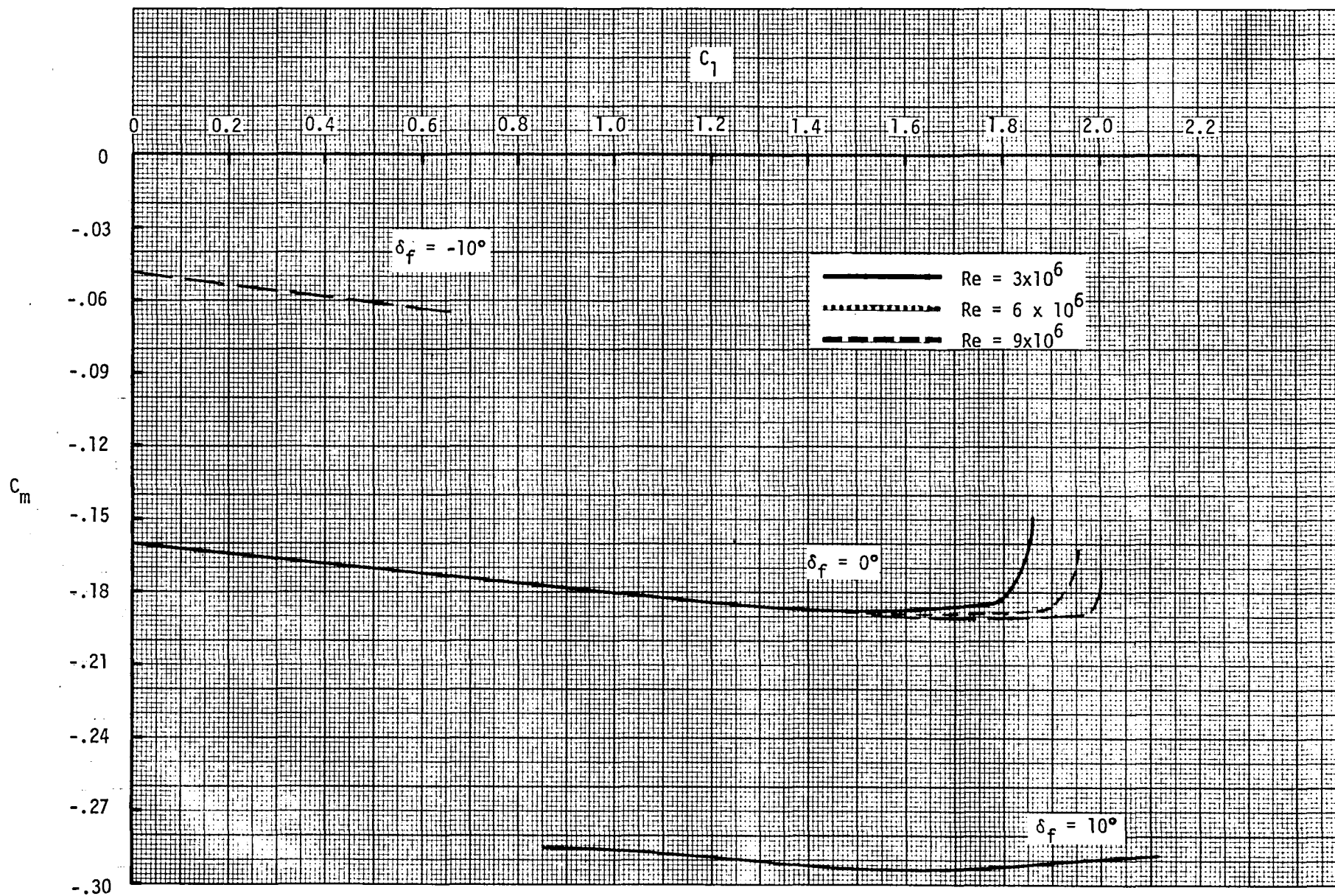
Figure 6. - The effect of lift coefficient (C_l) on the
variation of pitching moment coefficient (C_m)
for several flap deflections and Reynolds numbers.
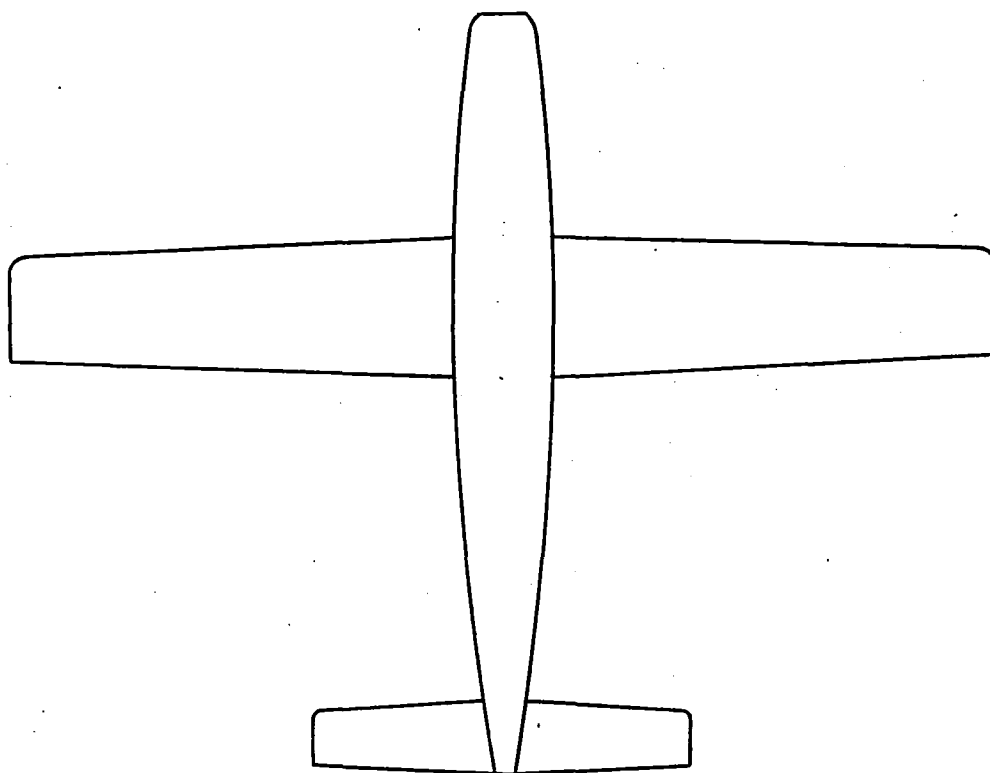
Figure 7. - The geometry of a typical aircraft
modeled on study.

R = 22.4"

18"
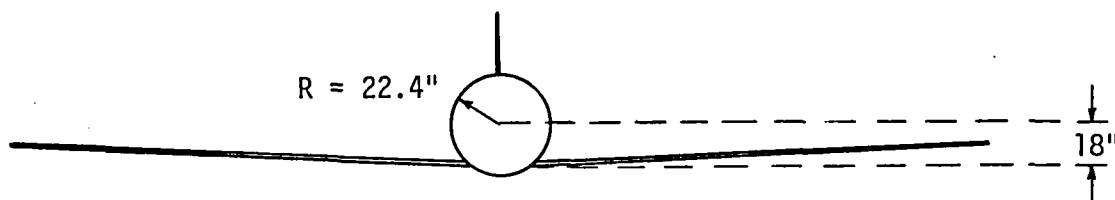
Figure 8. - Front view of aircraft modeled in study.
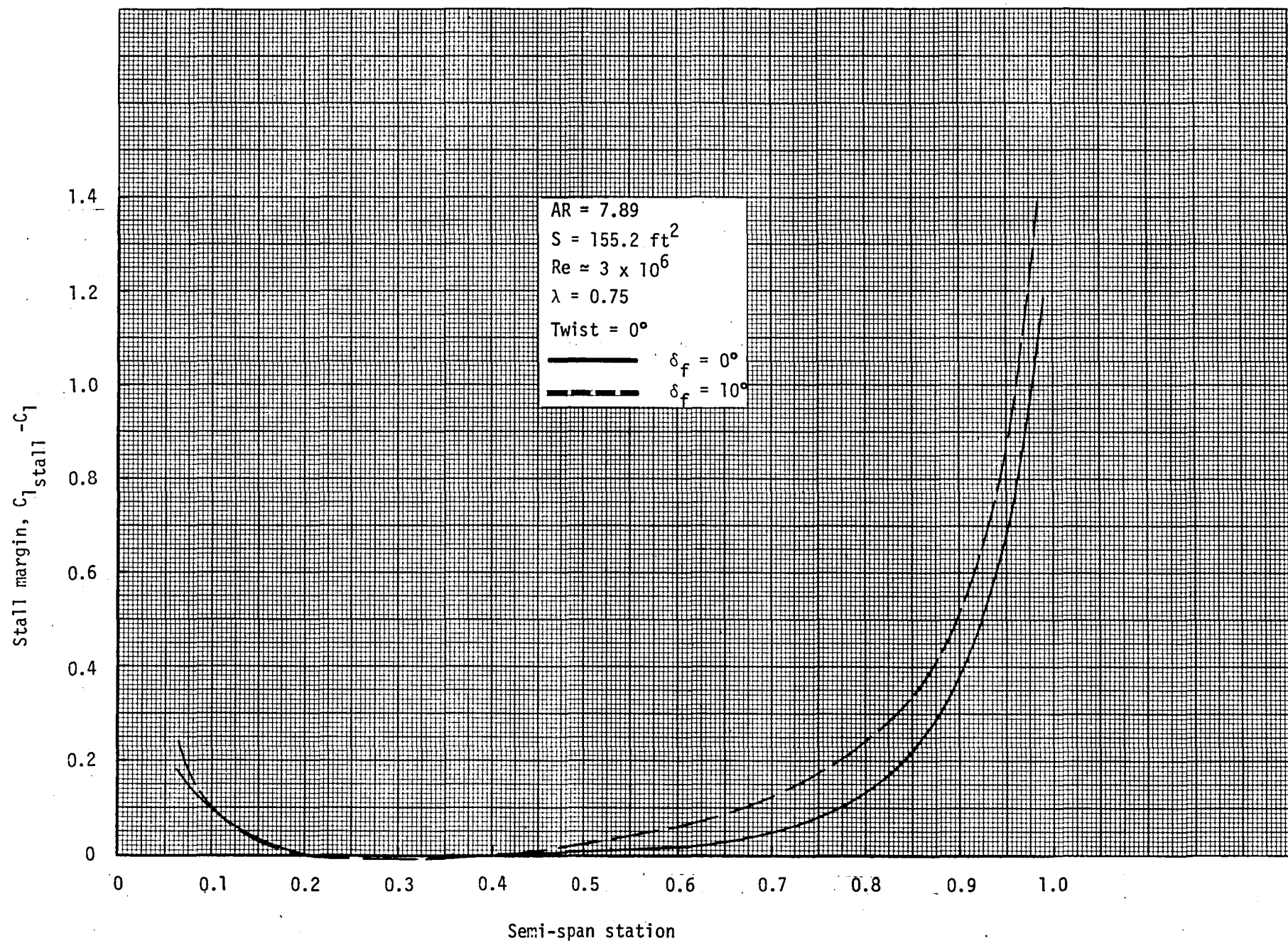
Figure 9. - The effect of flap deflections on the stall margin distribution.
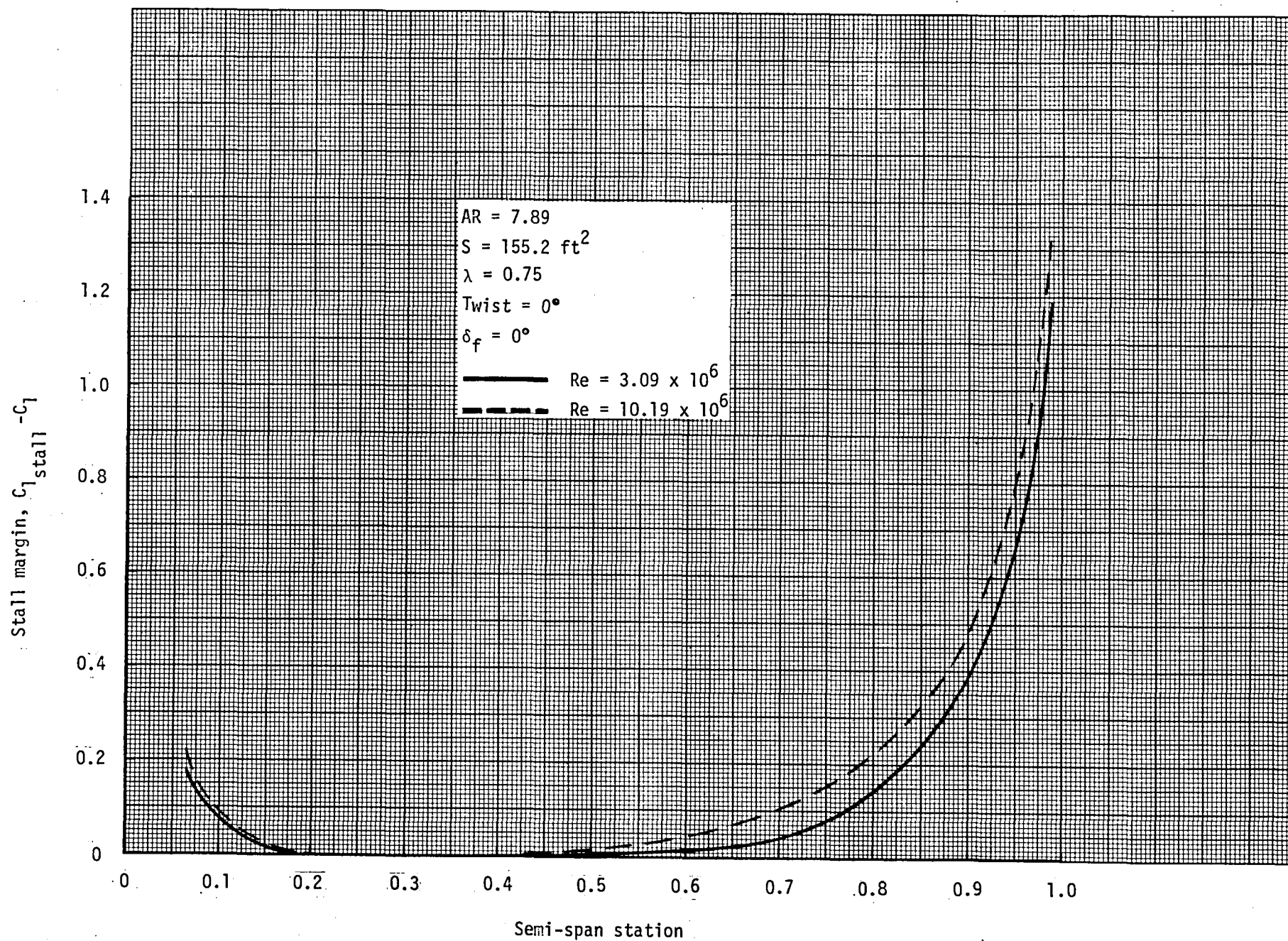
Figure 10. - The effect of Reynolds Numbers on the stall margin distribution.
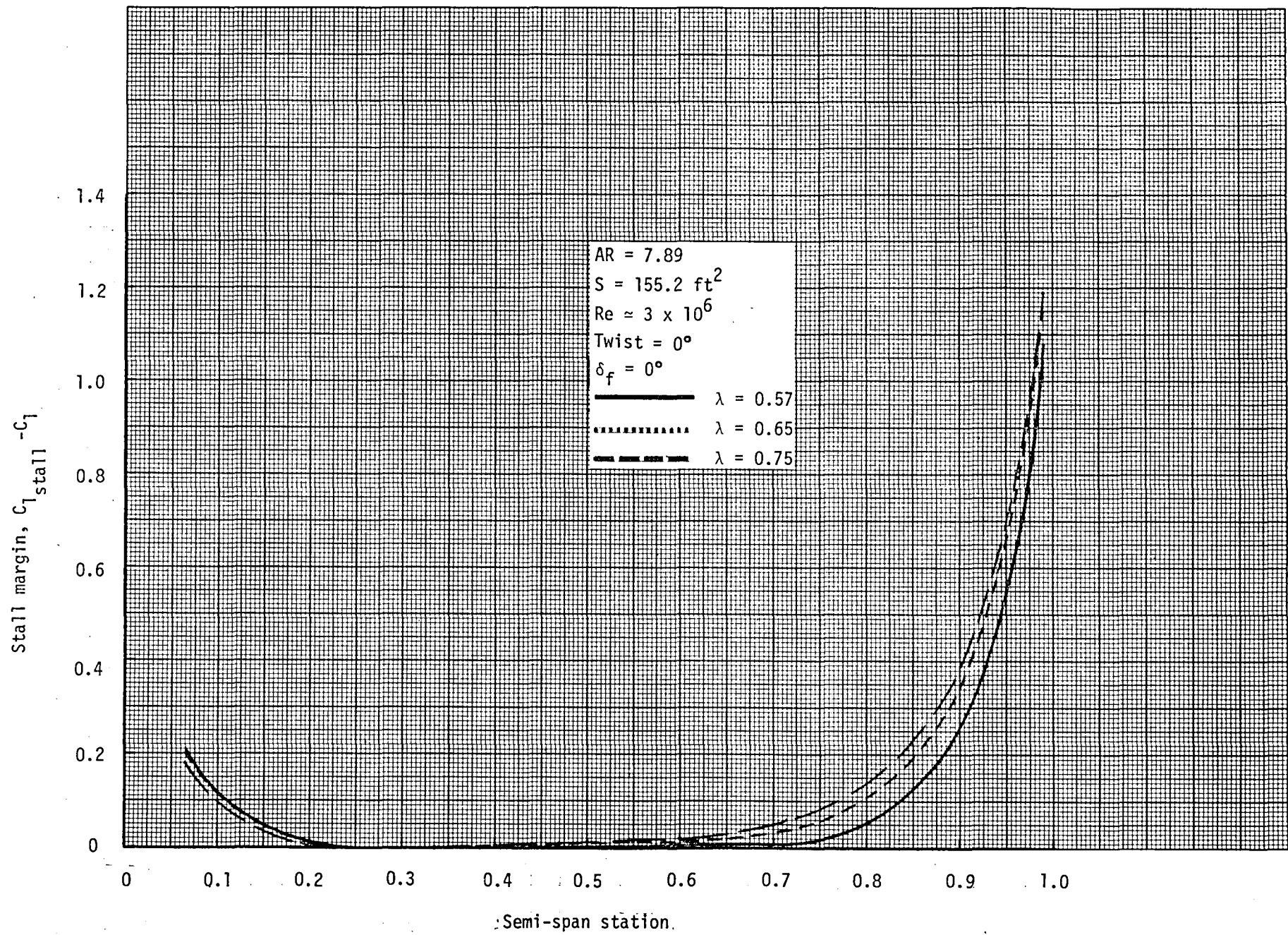
Figure 11. - The effect of taper on the stall margin distribution.
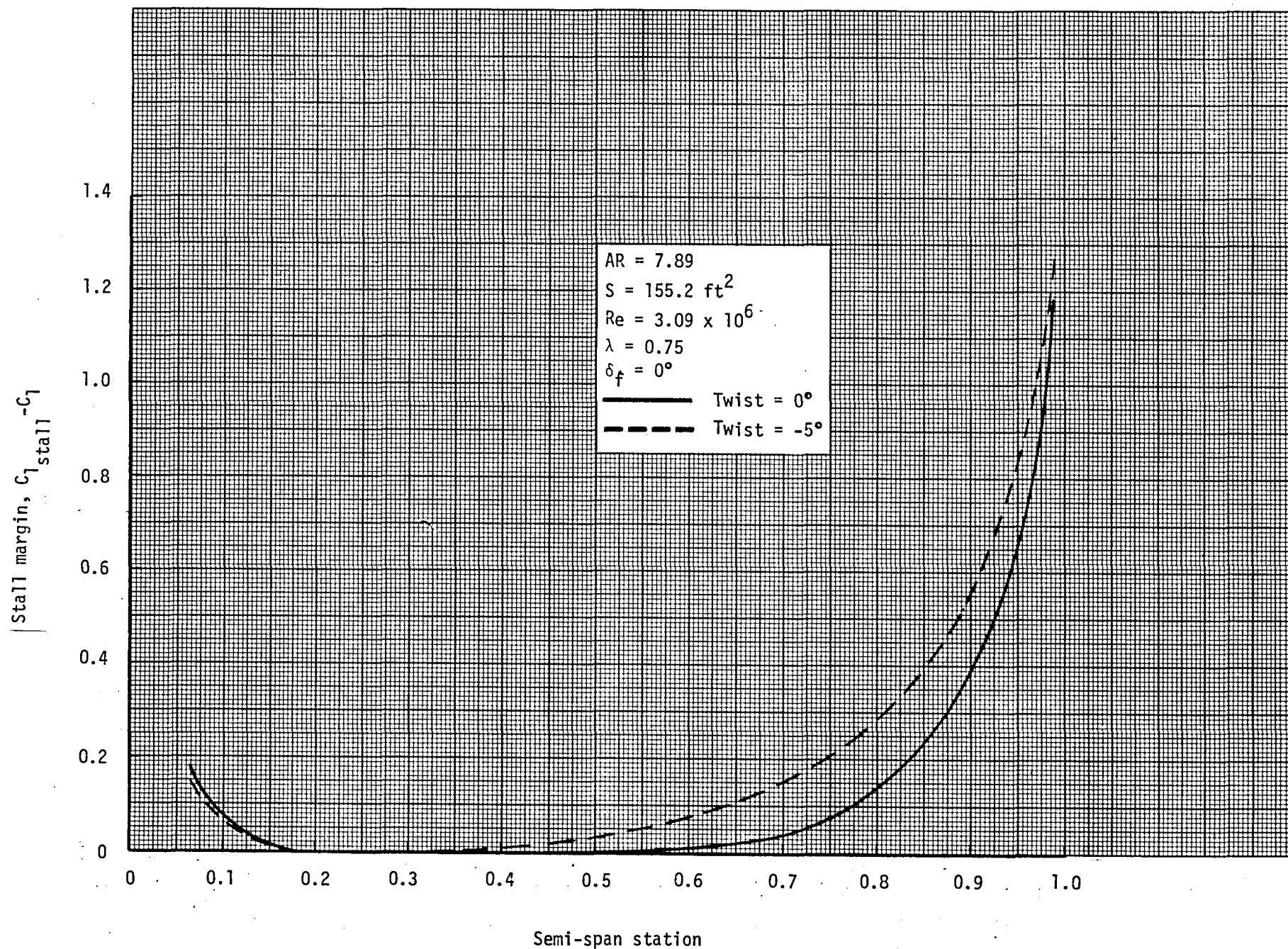
Figure 12. - The effect of twist on the stall margin distribution.
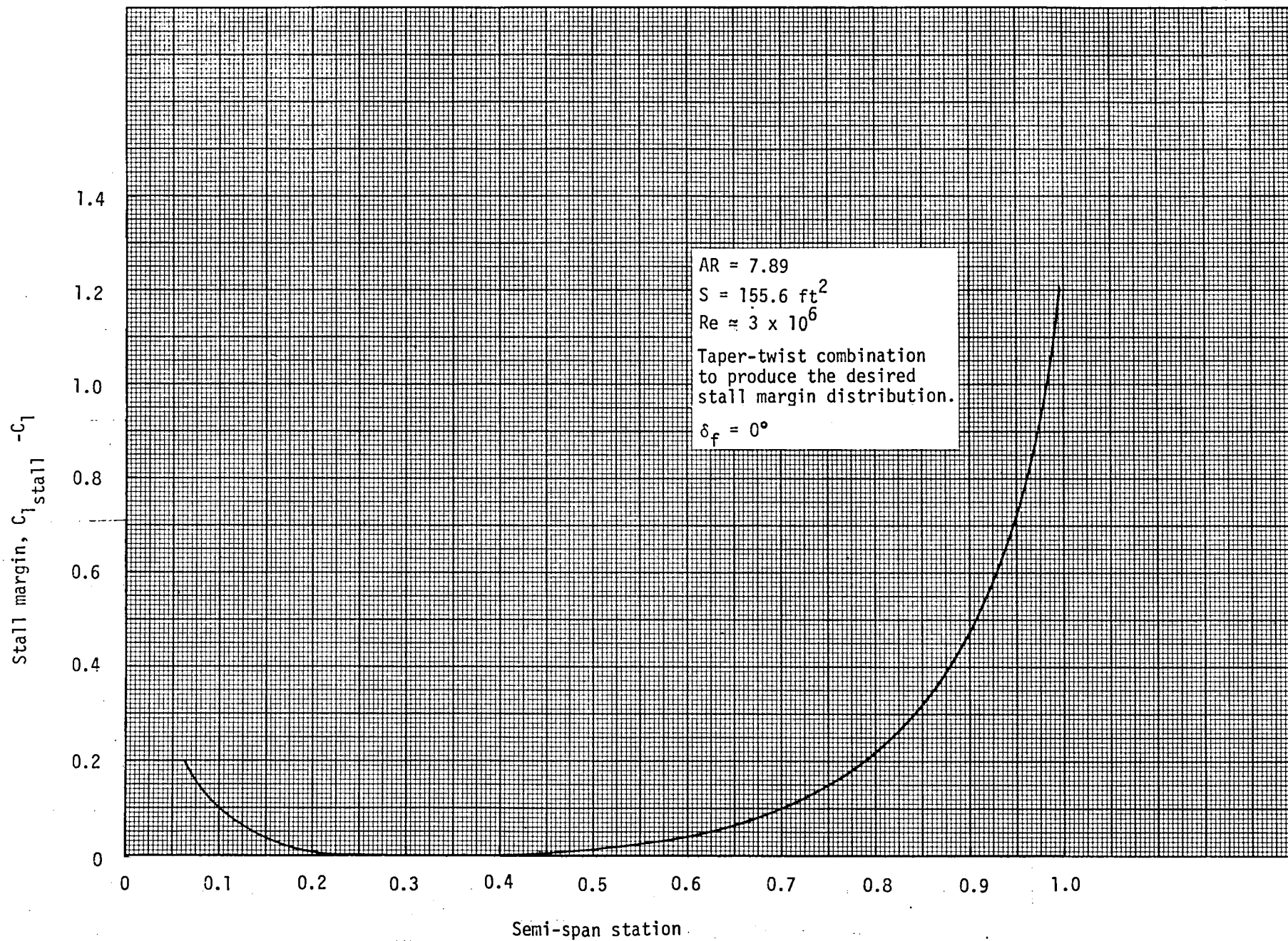
Figure 13. - The desired stall margin distribution.
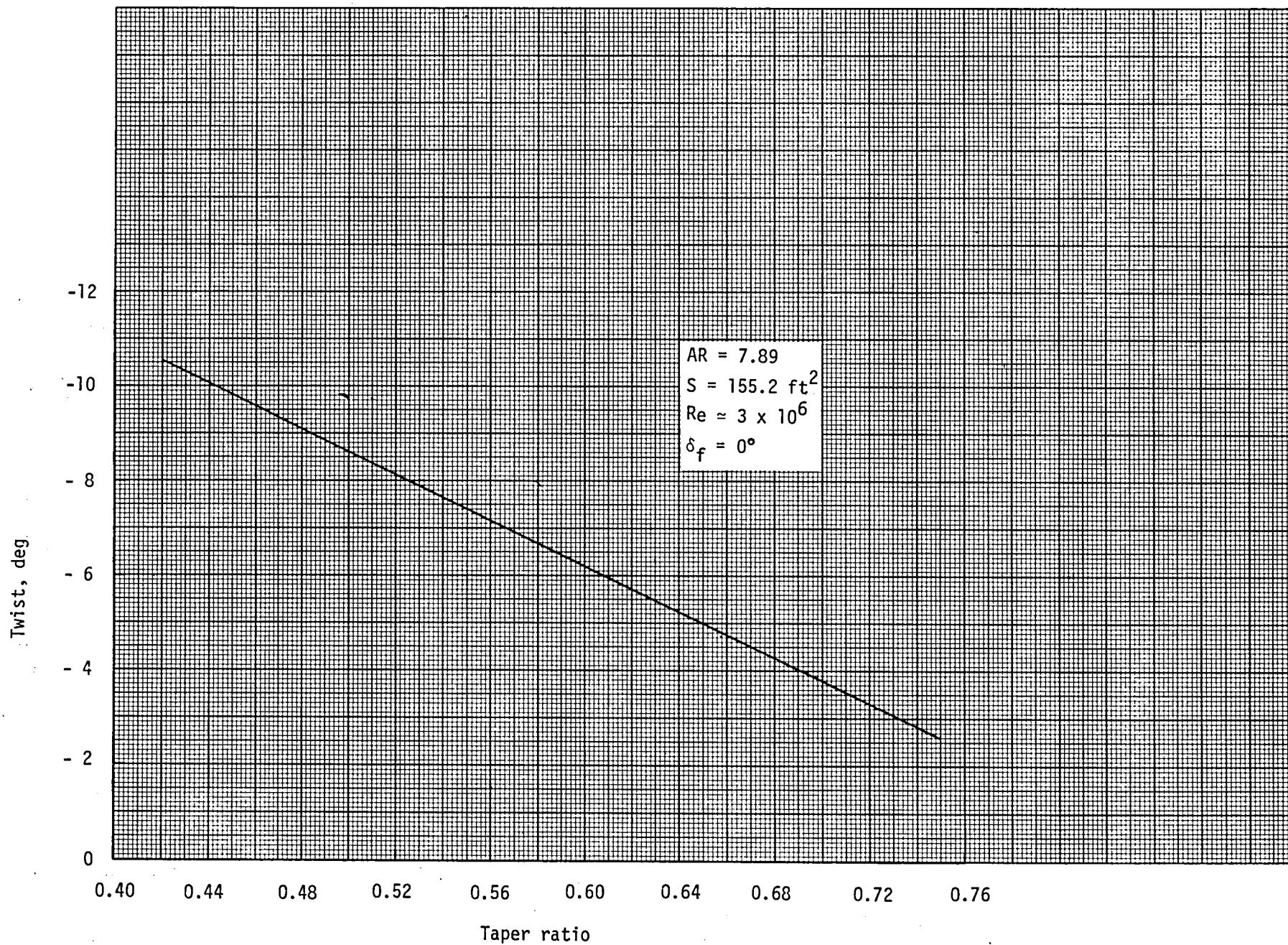
Figure 14. - Taper-twist combinations required to produce the desired
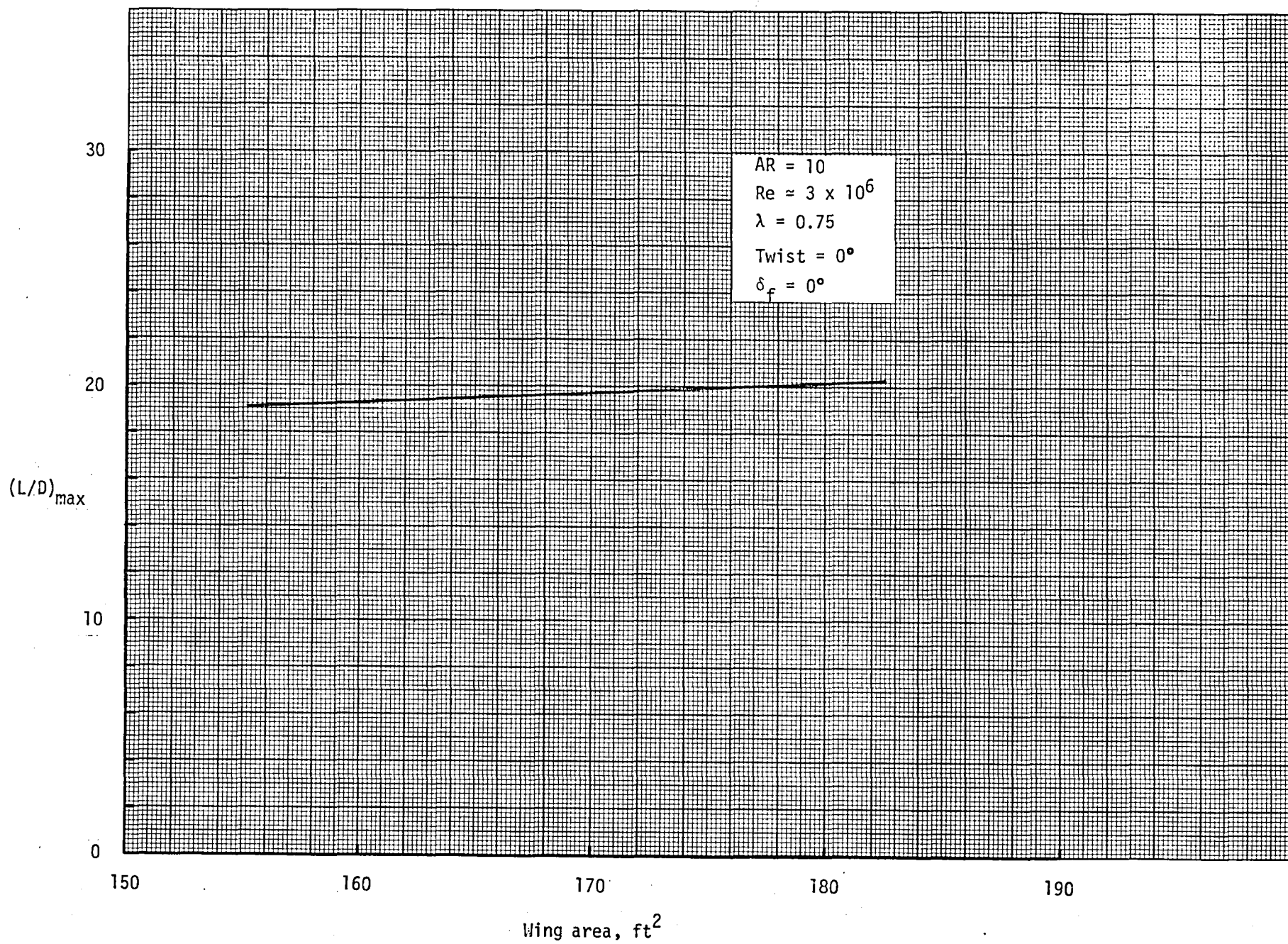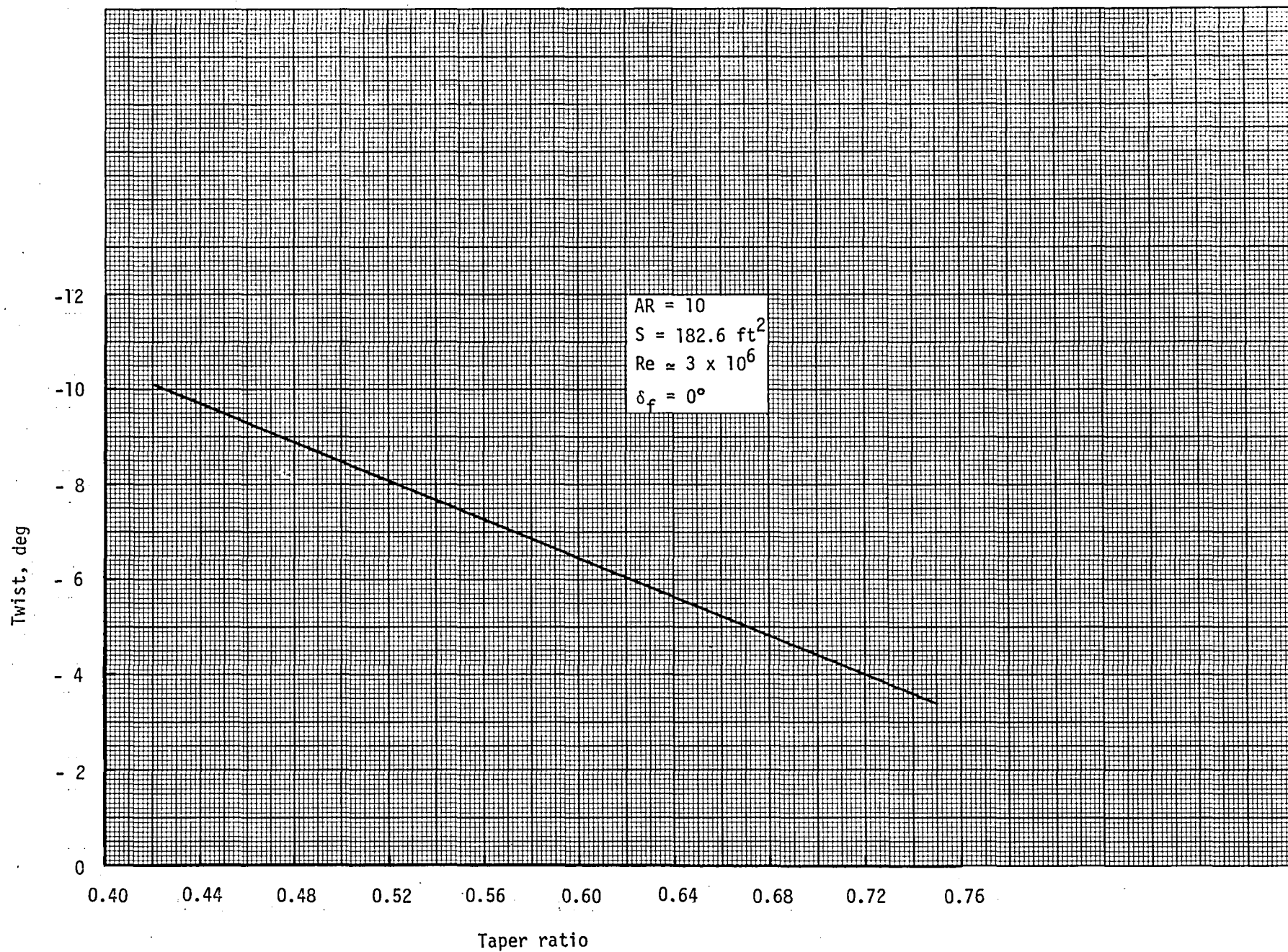stall margin distribution for wings with AR = 7.89 and S = 155.2 ft^2.
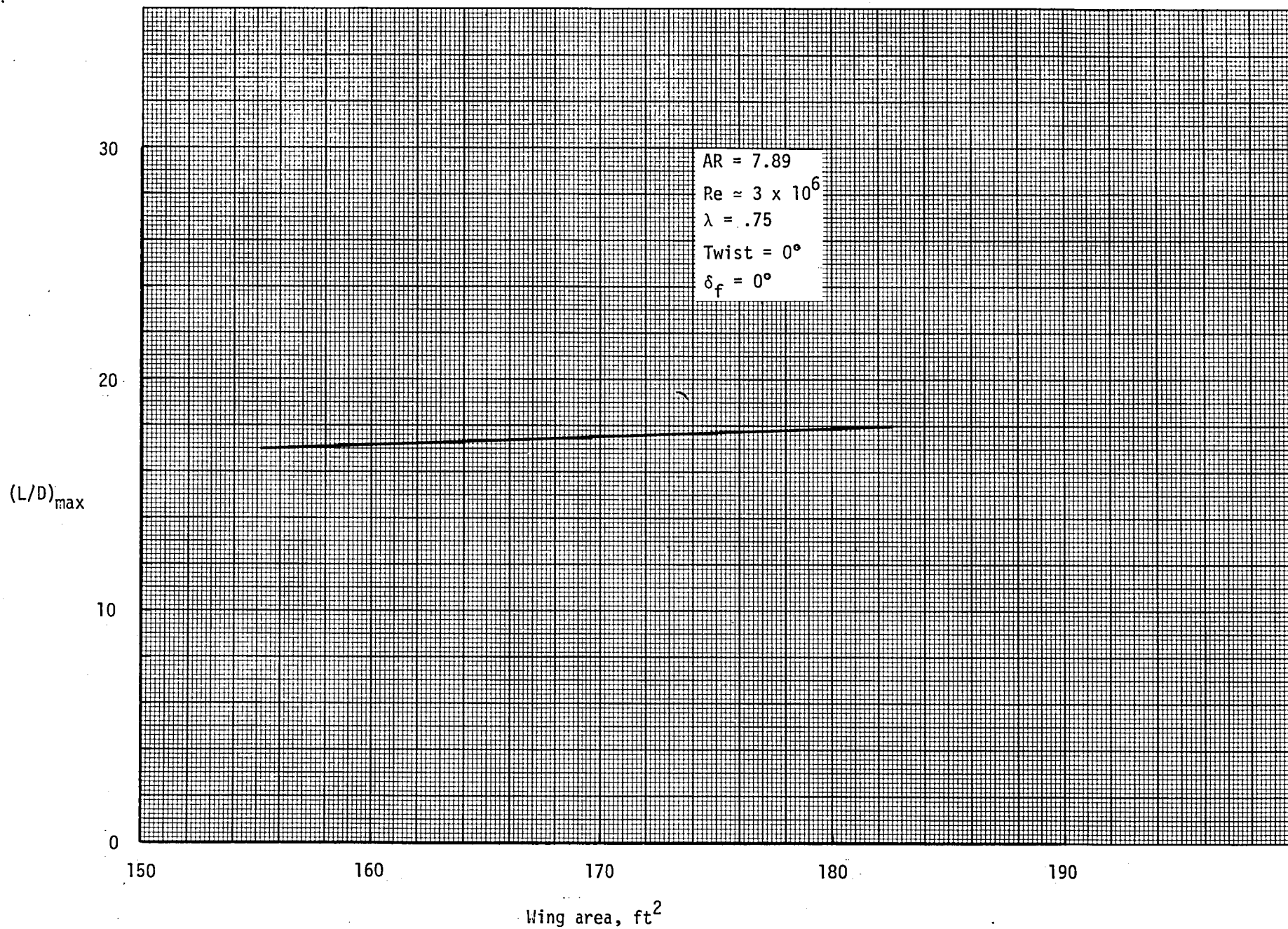
Figure 15. - $(L/D)_{max}$ as a function of S for AR = 7.89.
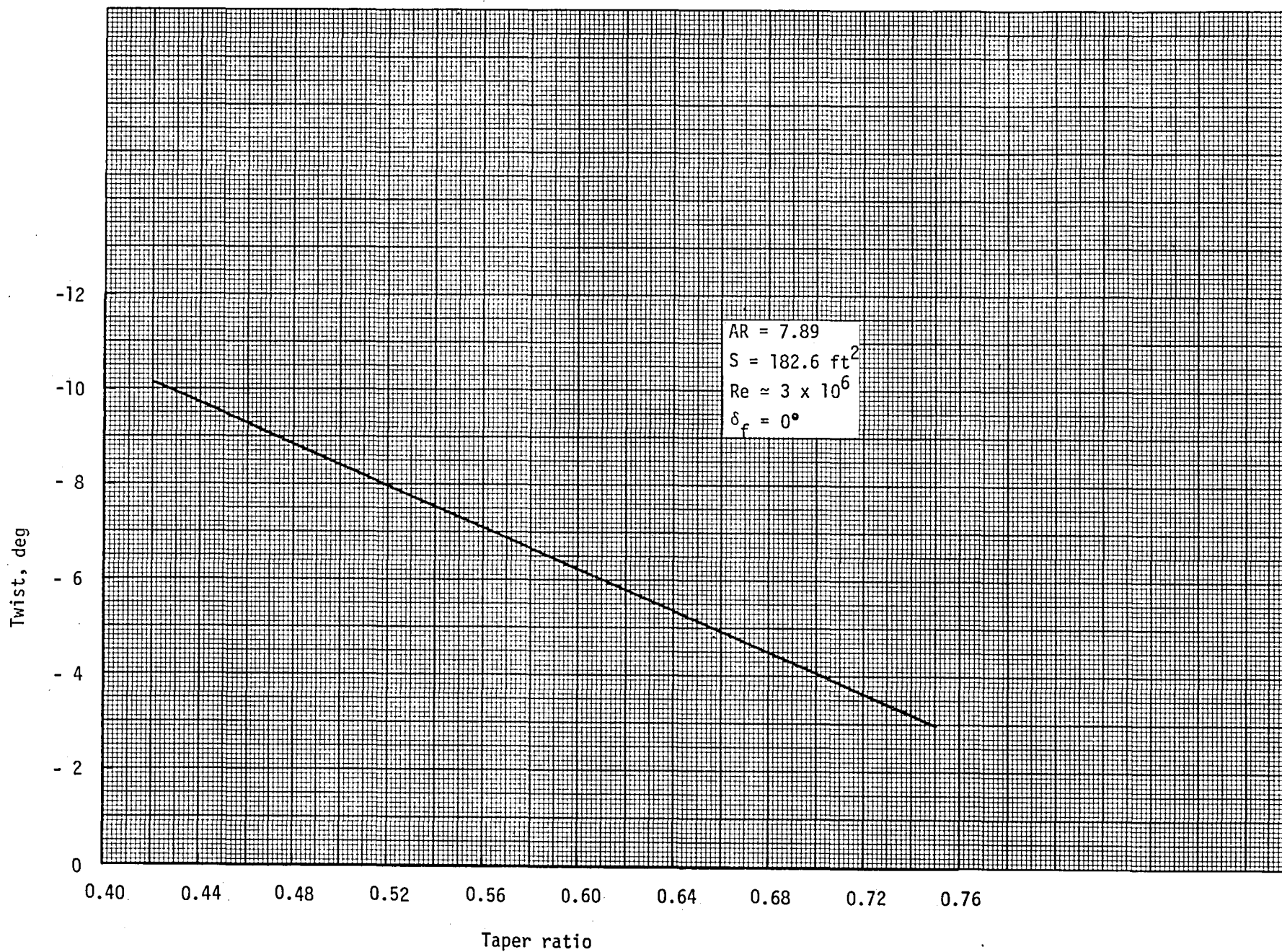
Figure 16. - Taper-twist combinations required to produce the desired stall margin distribution for wings with AR = 7.89 and S = 182.6 ft^2.
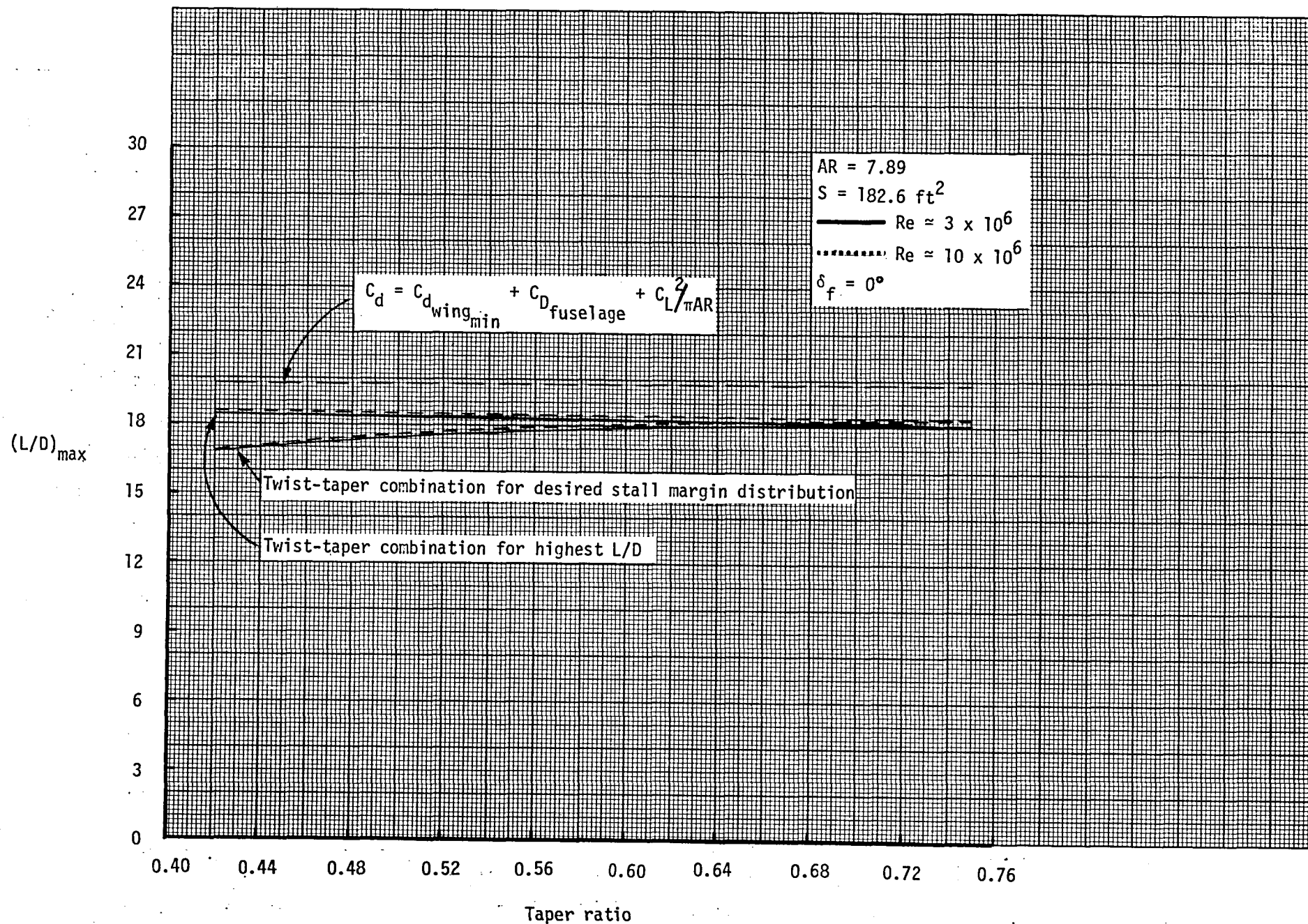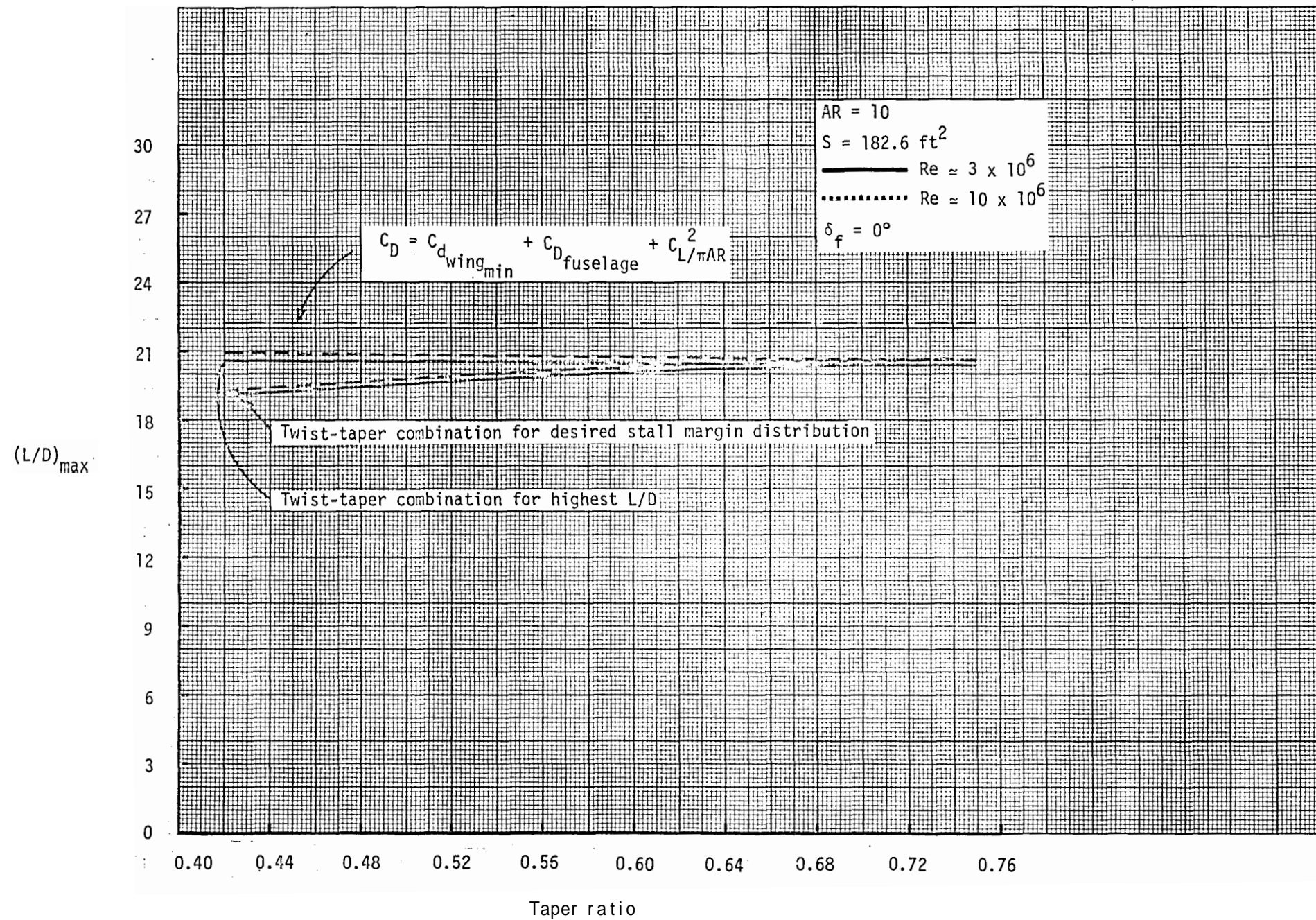
Figure 17. - $(L/D)_{max}$ as a function of taper for $S = 182.6$ ft^2 and AR = 7.89.
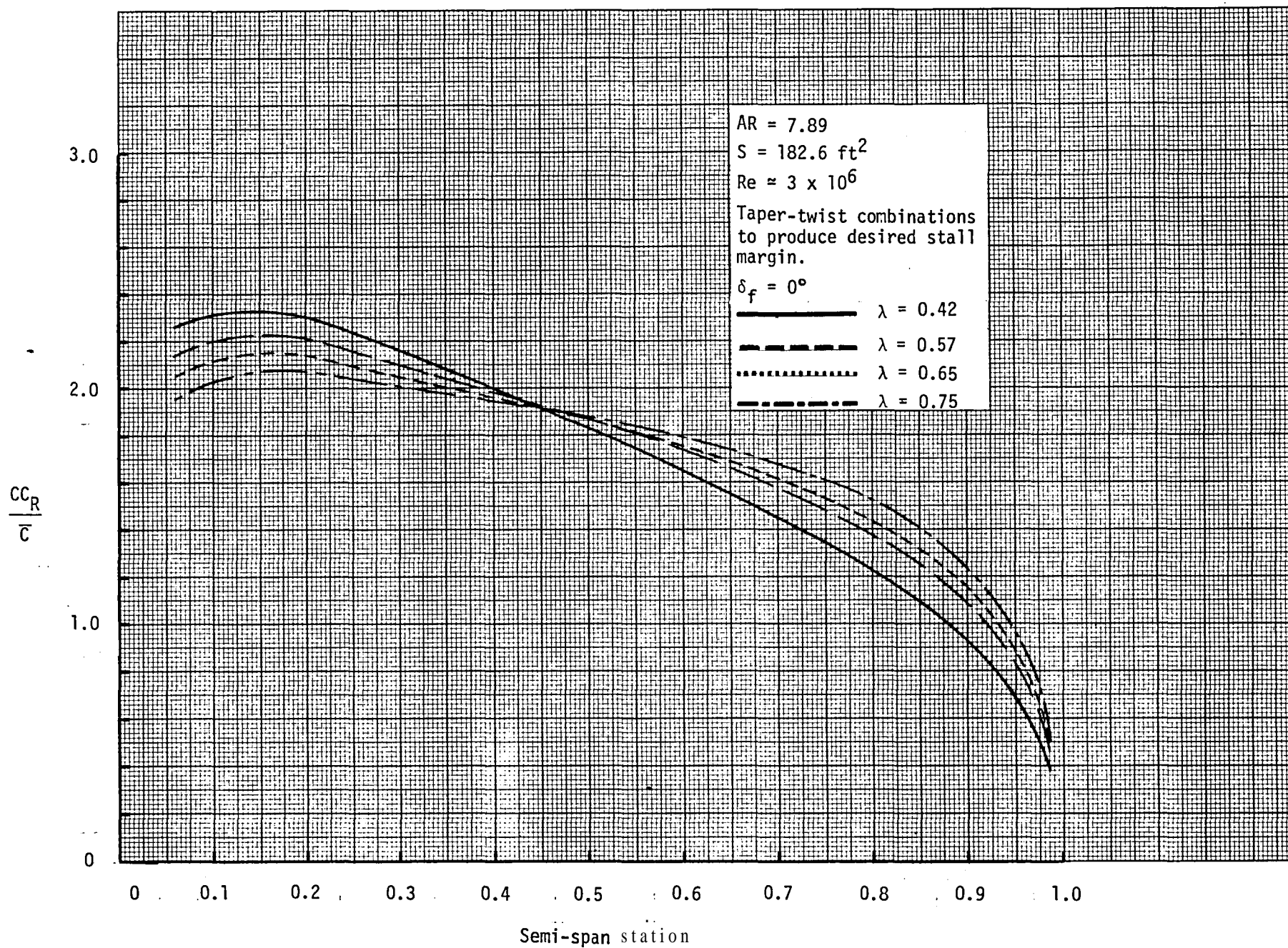
Figure 18. - Variations in the wing span load distribution with changes in taper.
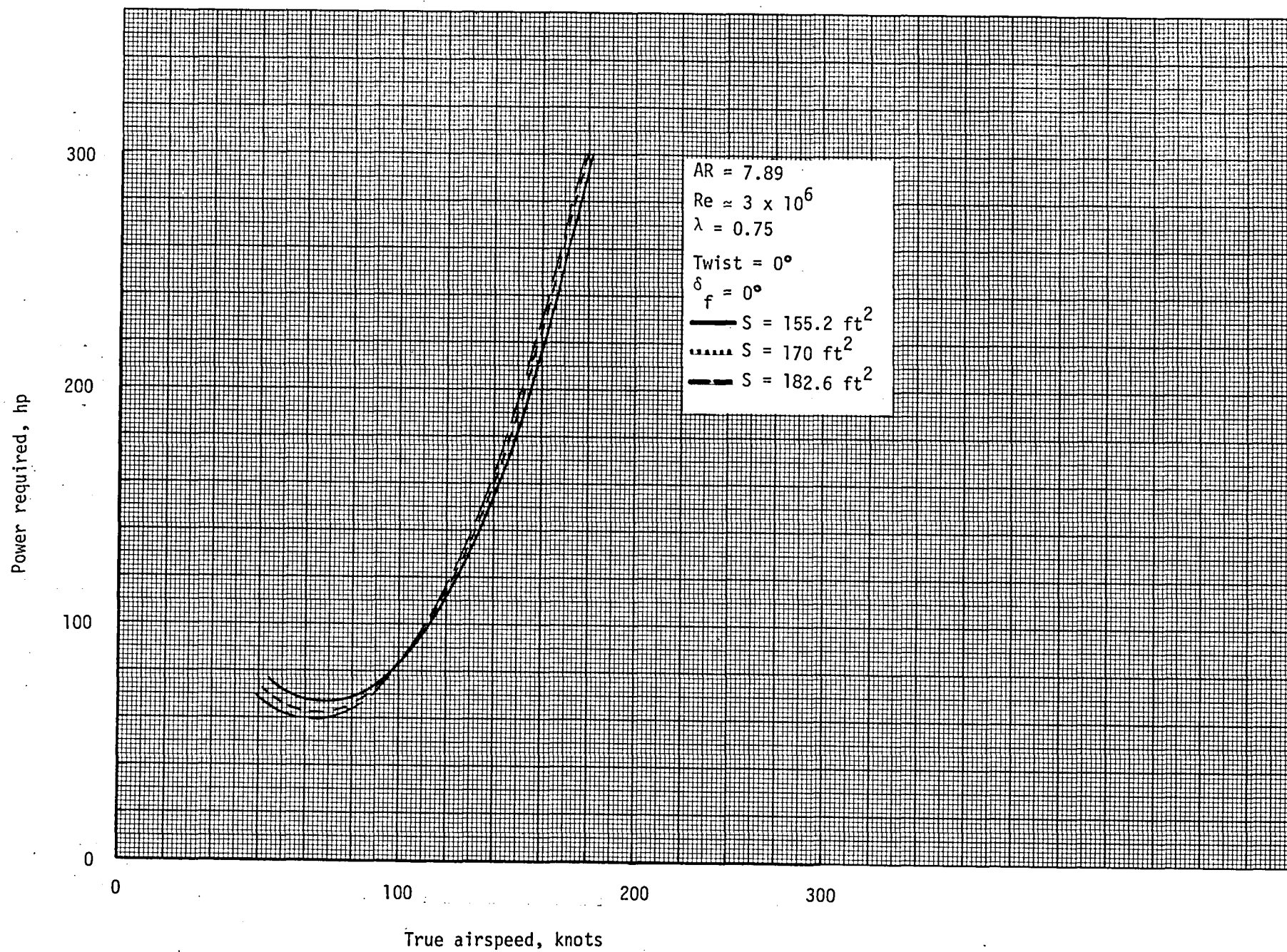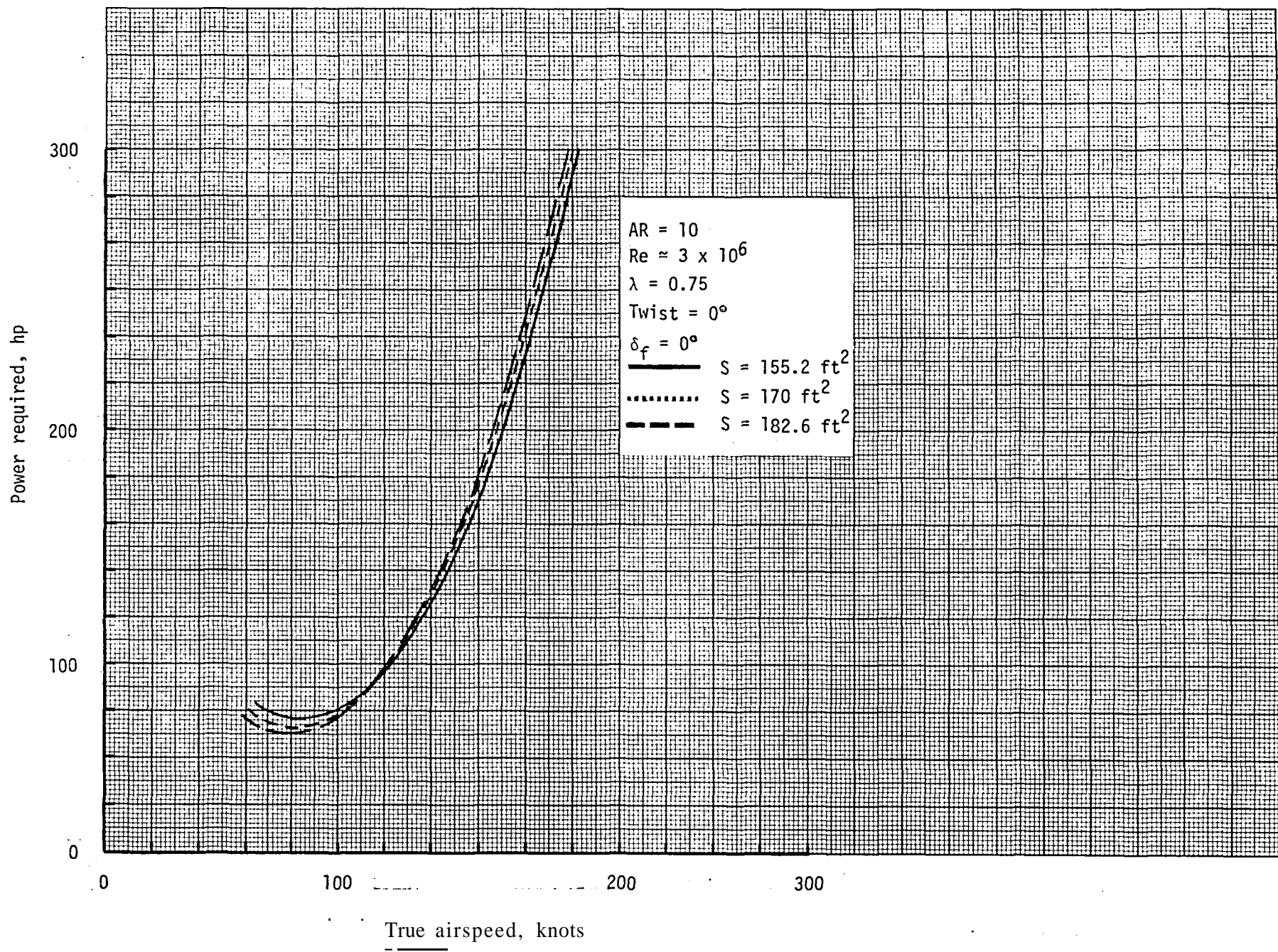
Figure 19. - Power vs. airspeed curves at sea level for AR = 7.89.
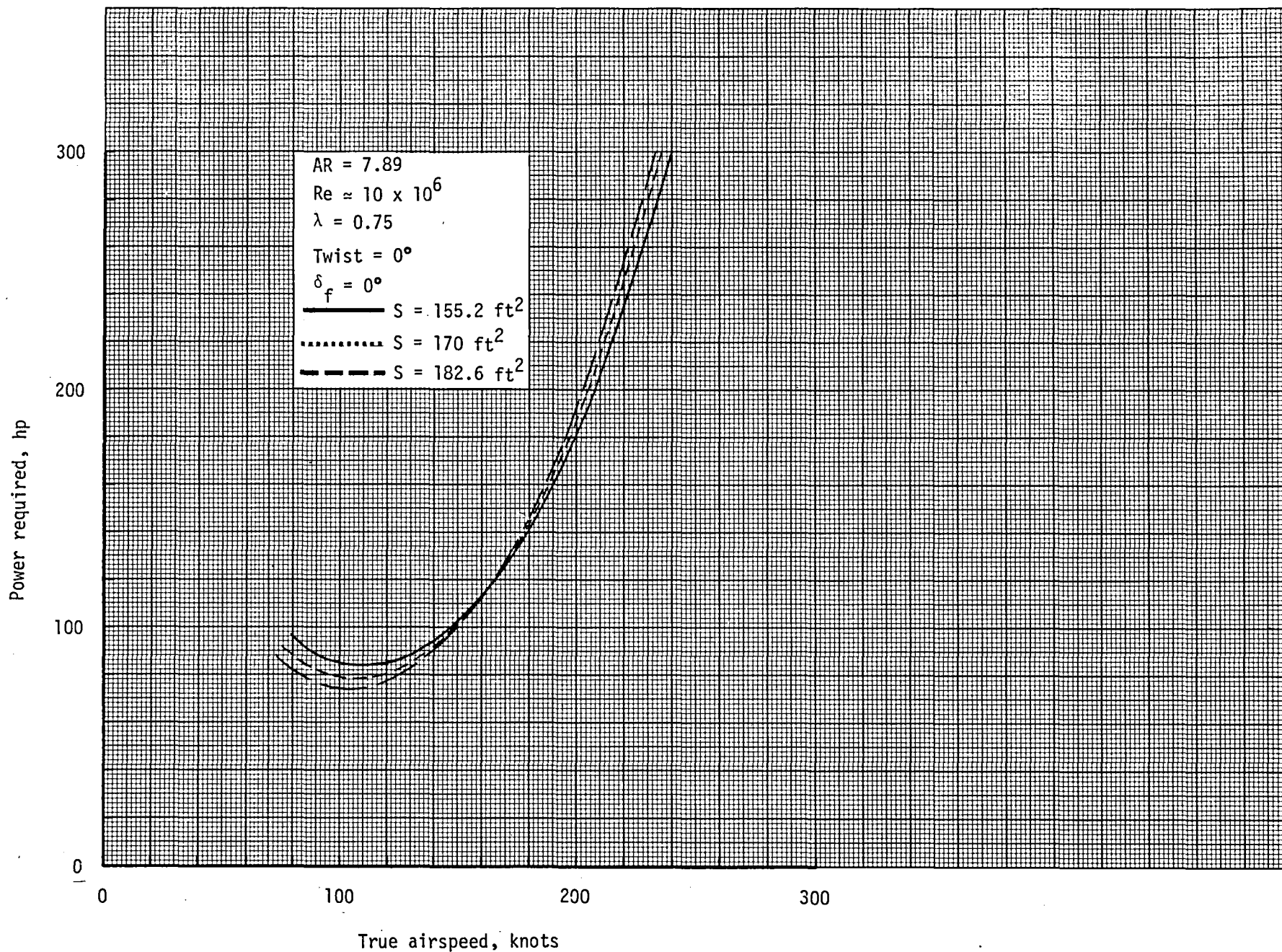
Figure 20. - Power vs. airspeed curves at h = 15,000 ft. for AR = 7.89.

Figure 21. - $(L/D)_{max}$ as a function of S for AR = 10.

Figure 22. - Taper-twist combinations required to produce the desired stall
margin distribution for wings with AR = 10 and S = 182.6 ft^2.

Figure 23. - $(L/D)_{max}$ as a function of taper for S = 182.6 ft^2 and AR = 10.

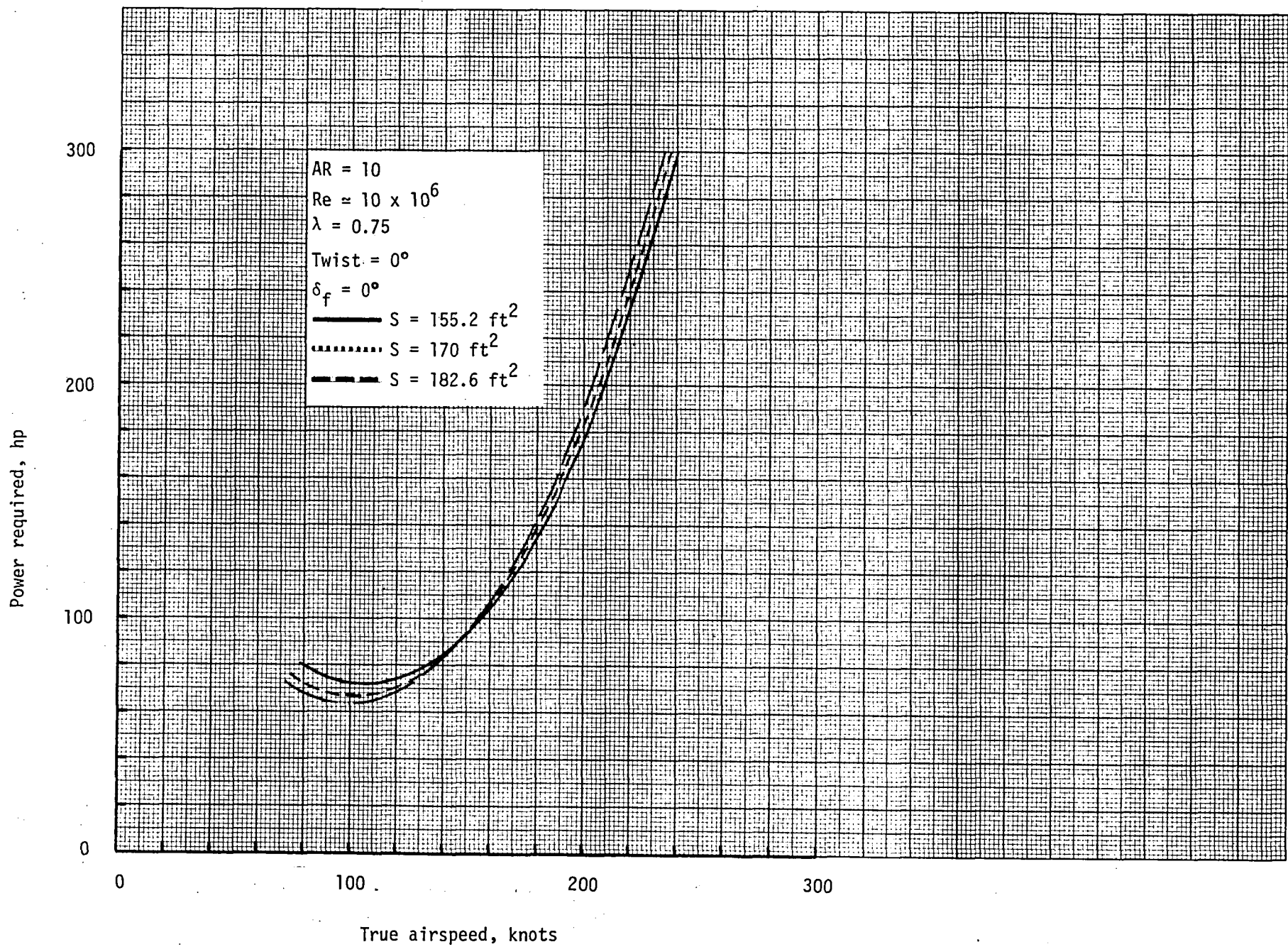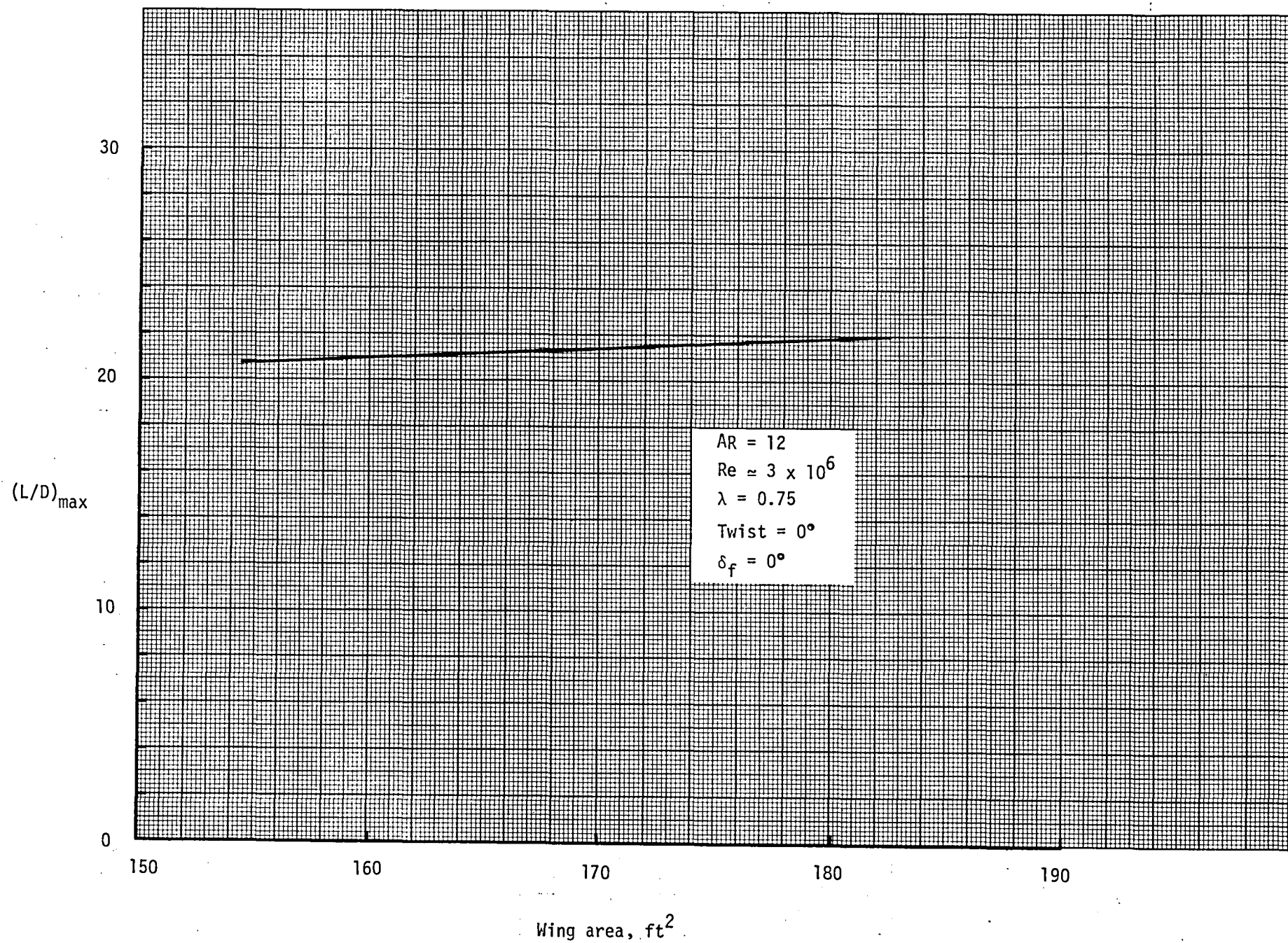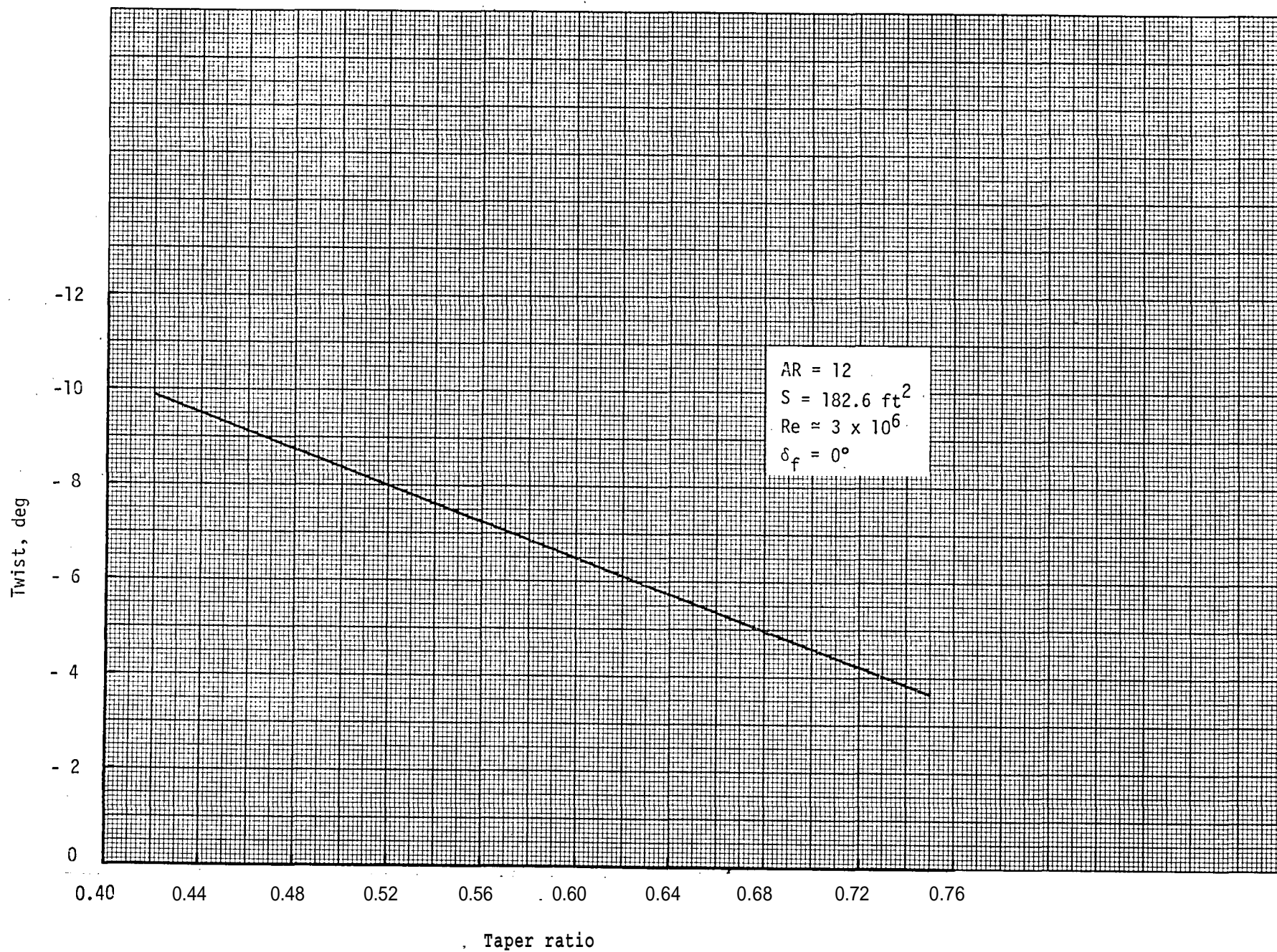Figure 24. - Power vs. airspeed curves at sea level for AR = 10.

Figure 25. - Power vs. airspeed curves at h = 15,000 ft. for AR =10.

The chart shows:

Power required, hp (vertical axis, 0 to 300)
True airspeed, knots (horizontal axis, 0 to 300)

Legend:
$AR = 10$
$Re \simeq 10 \times 10^6$
$\lambda = 0.75$
Twist $= 0°$
$\delta_f = 0°$
——— $S = 155.2$ ft^2
.... $S = 170$ ft^2
— — — $S = 182.6$ ft^2

Figure 26. - $(L/D)_{max}$ as a function of S for AR = 12.

Figure 27. — Taper-twist combinations required to produce the desired stall
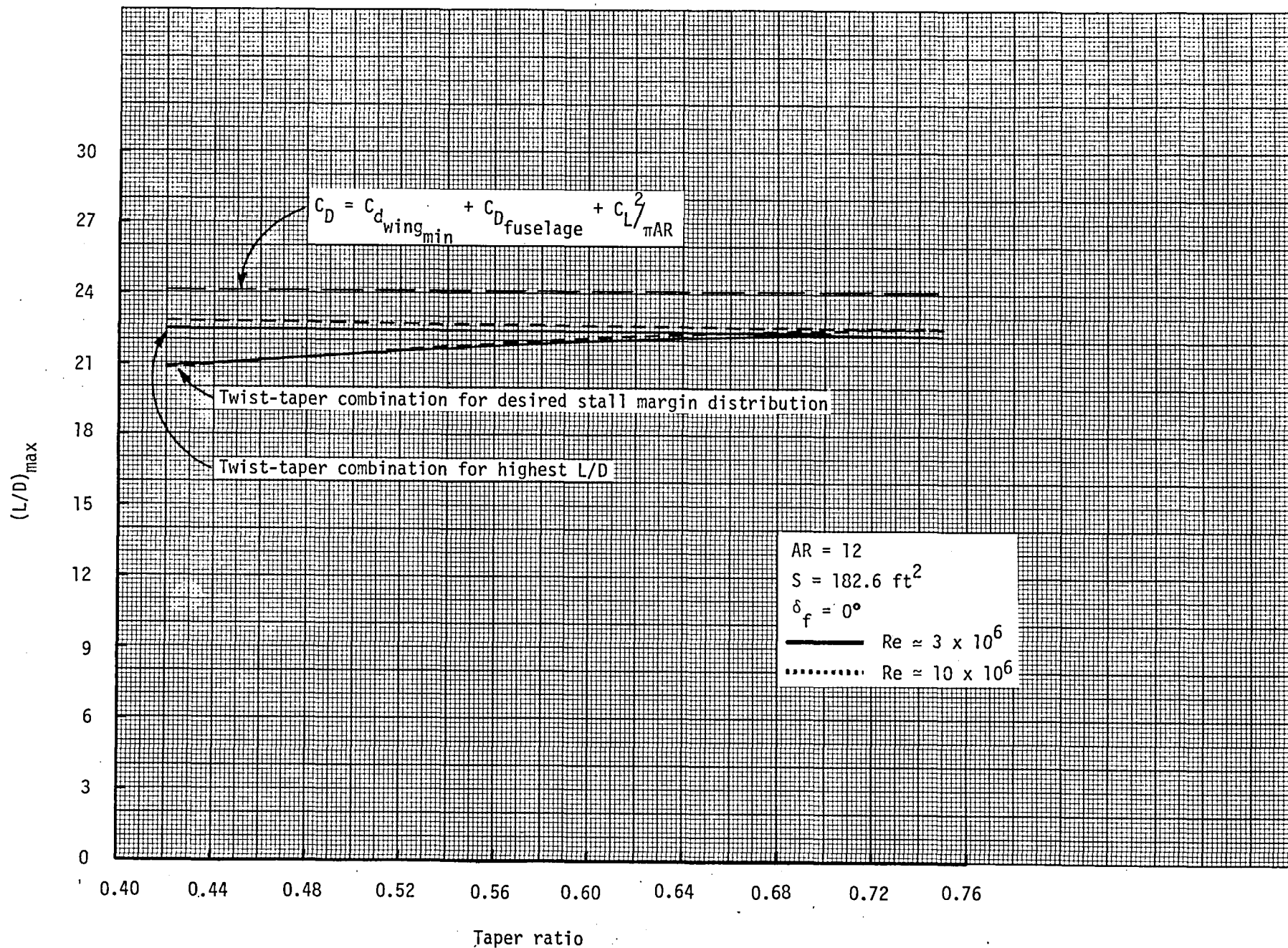margin distribution for wings with AR = 12 and S = 182.6 ft².

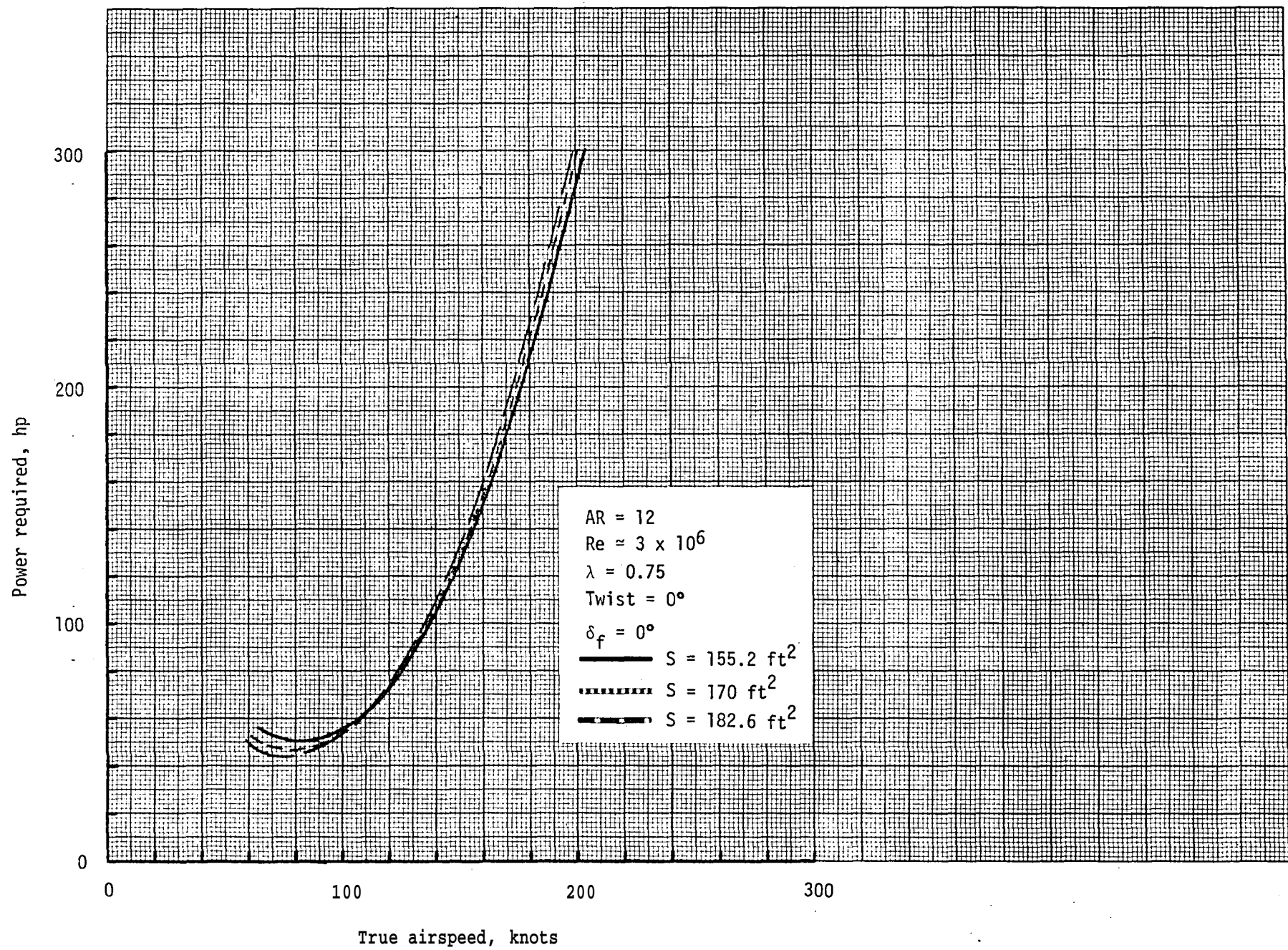Figure 28. - $(L/D)_{max}$ as a function of taper for $S = 182.6$ ft^2 and $AR = 12$.

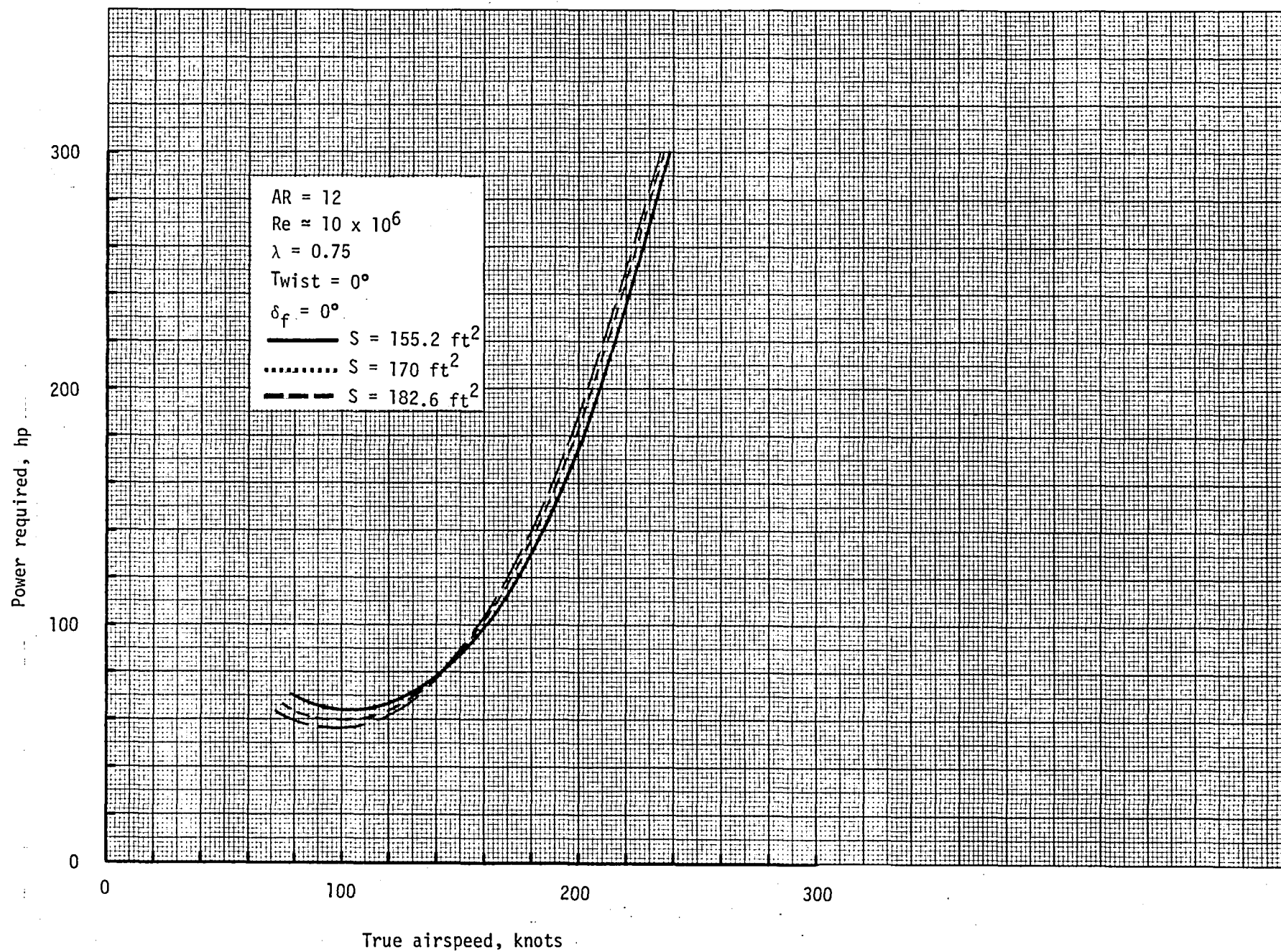Figure 29. - Power vs. airspeed curves at sea level for AR = 12.

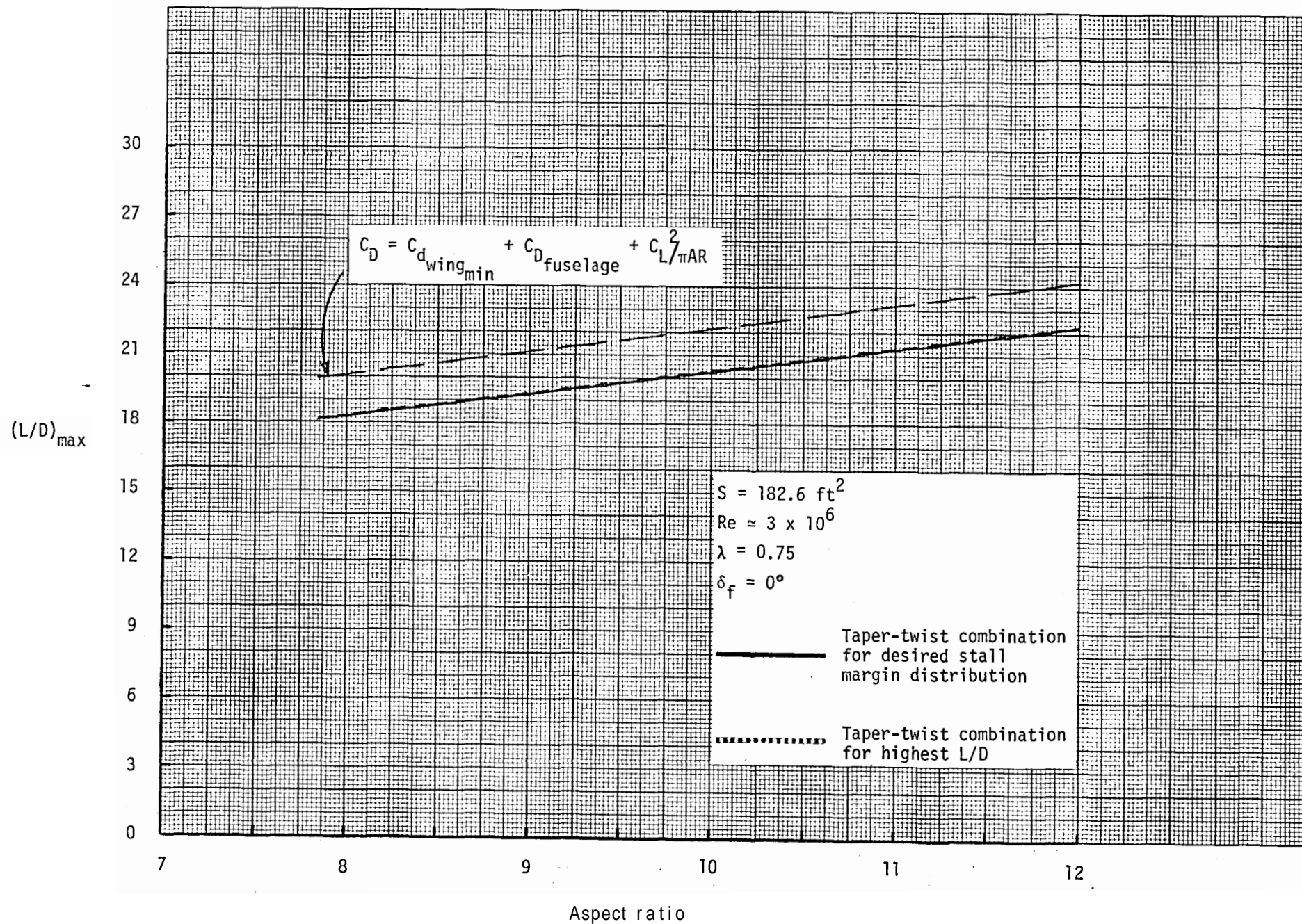Figure 30. - Power vs. airspeed curves at h = 15,000 ft. for AR = 12.

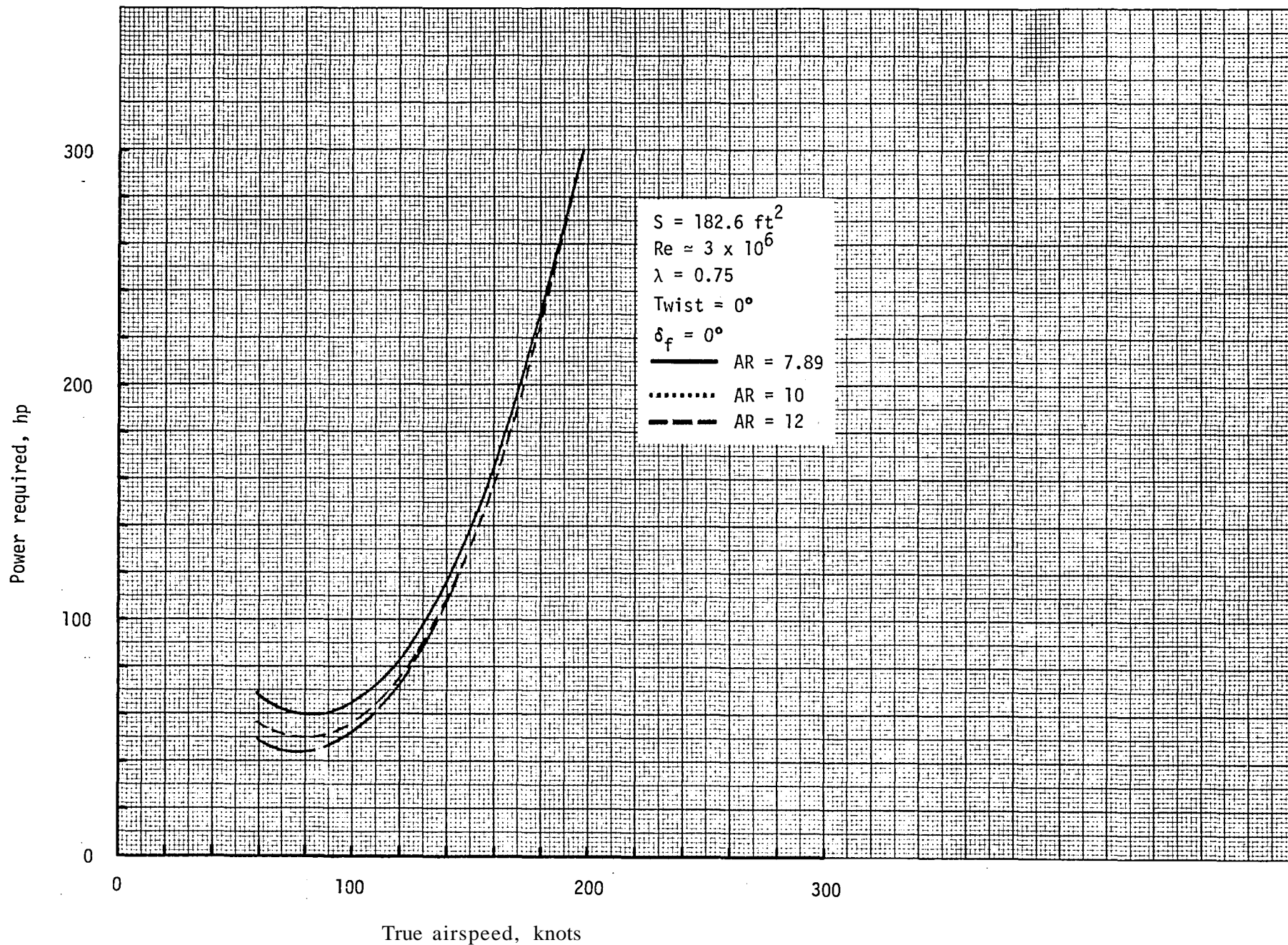Figure 31. - $(L/D)_{max}$ as a function of AR for S = 182 ft^2.

Figure 32. - The effect of AR on the power vs. airspeed curves at sea level.

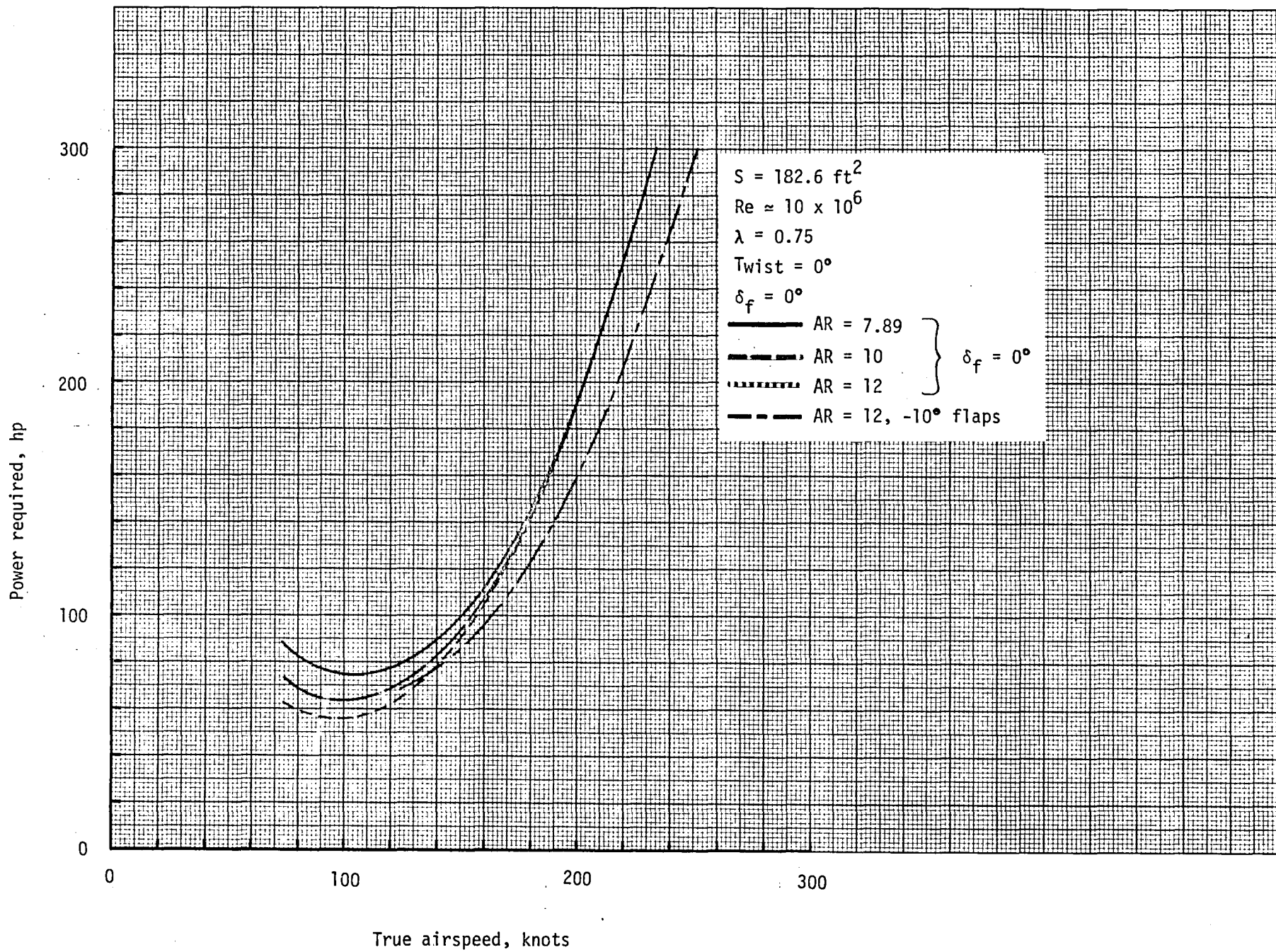Figure 33. - The effect of AR on the power vs. airspeed curves at h = 15,000 ft.

1. Report No. NASA TM-80154	2. Government Accession No.	3. Recipient's Catalog No.
4. Title and Subtitle A PARAMETRIC WING DESIGN STUDY FOR A MODERN LAMINAR FLOW WING		5. Report Date December 1979
		6. Performing Organization Code
7. Author(s) John A. Koegler, Jr.		8. Performing Organization Report No.
		10. Work Unit No.
9. Performing Organization Name and Address NASA Langley Research Center Hampton, VA 23665		11. Contract or Grant No.
		13. Type of Report and Period Covered Technical Memorandum
12. Sponsoring Agency Name and Address National Aeronautics and Space Administration Washington, DC 20546		14. Army Project No.

15. Supplementary Notes

16. Abstract

This report presents the results of a parametric wing design study using the NL(S)-0715F airfoil, a modern laminar flow section. The wings were designed to exhibit desirable stall characteristics while maintaining high cruise performance. It was found that little is sacrificed in cruise performance when satisfying the stall margin requirements if a taper ratio of 0.65 or greater is used. When choosing a taper ratio, however, it must be remembered that the outboard wing loading and thus the wing root bending moment grows with increasing taper ratio.

17. Key Words (Suggested by Author(s)) Laminar Flow Stall Performance	18. Distribution Statement Unclassified – Unlimited Subject Category 02		
19. Security Classif. (of this report) Unclassified	20. Security Classif. (of this page) Unclassified	21. No. of Pages 42	22. Price* $4.50